

Comparative interevent time statistics of degassing and seismic activity at Villarrica Volcano (Chile)

Johanna Lehr¹, Stefan Bredemeyer^{2,3}, Wolfgang Rabbel¹, Martin Thorwart¹,
Luis Franco-Marín⁴

¹Kiel University

²GEOMAR Helmholtz Centre for Ocean Research Kiel, Kiel, Germany

³GFZ German Research Centre for Geosciences, Potsdam, Germany

⁴Observatorio Volcanológico de los Andes del Sur (OVDAS), Servicio Nacional de Geología y Minería (SERNAGEOMIN), Temuco, Chile

Key Points:

- We compare the statistical distribution of time intervals between of explosive and volcano-tectonic seismic signals and degassing events.
- Normalized distributions of explosions and degassing events are surprisingly similar despite different orders of magnitude of time scales.
- Their interplay was modeled as a renewal process.

Plain Language Summary

[enter your Plain Language Summary here or delete this section]

Corresponding author: Johanna Lehr, johanna.lehr@ifg.uni-kiel.de

Abstract

It is generally assumed that seismic activity at volcanoes is closely connected to degassing processes. Intuitively, one would therefore expect a good correlation between degassing rates and seismic amplitude. However, both examples and counterexamples of such a correlation exist. In this study on Villarrica volcano (Chile), we pursued a different approach to relate gas flux and volcanic seismicity using 3 months of SO₂ flux rate measurements and 12 days of seismic recordings from early 2012. We analyzed the statistical distributions of interevent times between transient seismic waveforms commonly associated with explosions and between peaks in the degassing time series. Both event types showed a periodic recurrence with a mode of 20-25 s and around 1 h for transients and degassing, respectively. The normalized interevent times were fitted by almost identical log-normal distributions. Given the actually very different time scales, this similarity potentially indicates a scale-invariant phenomenon. We could reproduce these empirical findings by modelling the occurrence of transients as a renewal process from which the degassing events were derived recursively with increasing probability since the previous degassing event. In this model, the seismic transients could be either produced by degassing processes within the conduit or by gas release at the lava lake surface while the longer intervals of the degassing events may be explained by accumulation of gas either in the magma column or in the juvenile gas plume. Additionally, we analyzed volcano-tectonic events, which behaved very differently from the transients. They showed the clustered occurrence of tectonic earthquakes.

1 Introduction

Villarrica Volcano is a highly active volcano in South America, which is known for its persistent seismic tremor and continuous degassing activity. Commonly, any seismic activity at a volcano is more or less directly attributed to the fluid dynamics within the plumbing system. Explosions are the violent releases of gas bubbles, while volcanic tremor and long-period (LP) events are frequently explained by moving gas, water or magma, that produce sustained reverberations along the walls of the conduits or pipes (Chouet, 1996). Even shear fractures (volcano-tectonic events) may be linked to changes in the pressure regime within the system which causes the opening (or closing) of new pathways for the fluids (Traversa & Grasso, 2010). Intuitively, one would thus expect a direct correlation between degassing and intensity of seismic activity.

The degassing activity of a volcano is, for example, efficiently monitored by measuring the SO₂ emission rate. Degassing magma releases SO₂ in considerable amounts, making it a good proxy for the amount of outgassed mass. The intensity of the seismicity is commonly indicated by a measure of the mean seismic amplitude such as the Real-time Seismic Amplitude Measurements (RSAM) which is the root-mean square of the seismic amplitude over a given time interval, typically 10 min or 24 h (Endo & Murray, 1991). Although positive correlations between RSAM and gas flux have been found at many volcanoes, there are some exceptions. An extensive overview was given by Salerno et al. (2018). These authors also proposed an explanation for this mismatch. They showed a generally good correlation between the weekly mean SO₂ flux and daily mean RSAM at Mt. Etna for two years of continuous data. The daily variations however correlated to a much lesser degree. For Villarrica, Palma et al. (2008) also established a largely good correlation between SO₂ emission rate and RSAM using data from 2000-2006. However, their data set was sparse. Mean flux rates for the correlation were obtained from a handful of daily measurements within 13 months; daily measurements consisted of 11 scans per day at most.

In this study we show continuous measurements of degassing rates recorded during daylight over three months at a rate of about one scan every 10 min using 3 scanning Mini-DOAS stations. Degassing and lava lake activity of Villarrica Volcano was ex-

69 ceptionally high throughout the entire study period (Global Volcanism Program, 2014).
70 During 10 days within this period, we also recorded the seismic activity close to the ac-
71 tive vent. At first, we compared the two data sets visually for correlations. However, no
72 correlation could be found whereupon we chose a statistical way to examine the relation-
73 ship. Instead of comparing the time series directly, we analyzed the interevent times be-
74 tween transient seismic events - commonly classified as explosions (Calder et al., 2004;
75 Ortiz et al., 2003; Palma et al., 2008) or long-period events (Richardson & Waite, 2013)
76 - and peaks in the degassing rate. This approach additionally mitigates the problem of
77 the different lengths between the observation periods.

78 After the introduction of Villarrica, an overview of interevent times and the un-
79 derlying concept of renewal processes in the context of seismology and volcanology is given.
80 In section 4, the data sets are introduced in detail. For the analysis of interevent times,
81 we distinguish three kinds of events: degassing events and two types of seismic events,
82 namely the transients and volcano-tectonic earthquakes. A vital part of this paper (sec-
83 tion 5.2) deals with the detection of different events and the compilation and complete-
84 ness of the catalogs. Subsequently, we model and compare the their distributions of in-
85 terevent times. In section 5.4, we propose a renewal process model to link the seismic-
86 ity and degassing fluctuation and to explain the striking similarity of their interevent times.
87 These distributions are contrasted with those of other volcanoes and of volcano-tectonic
88 earthquakes from Villarrica.

89 2 Villarrica volcano

90 Villarrica is a 2847 m high, glacier-covered stratovolcano of basaltic to basaltic-andesitic
91 composition, located in the Chilean Andes. It is one of the most active and dangerous
92 volcanoes in South America. The volcanic activity consists of persistent degassing and
93 occasional periods of mild explosive activity including ash and lava emissions (Global
94 Volcanism Program, 2013).

95 The central vent hosts an active lava lake. Its depth varies more or less periodi-
96 cally by about 100 m within a few days (Richardson et al., 2014). Degassing activity at
97 the lake surface was described in detail by Palma et al. (2008) and includes seething, bub-
98 ble bursting and occasionally Strombolian explosions and lava fountains. Analysis of MODIS
99 satellite data showed an elevated level of radiated heat throughout 2010-2012 (Global
100 Volcanism Program, 2014), which was particularly enhanced during the period consid-
101 ered in this work.

102 The seismic activity is mainly characterized by a persistent tremor and extended
103 periods of days to weeks during which short, transient bursts occur in approximately 1-
104 min intervals (Ortiz et al., 2003; Calder et al., 2004; Palma et al., 2008). The latter are
105 commonly ascribed to explosive activity. Interestingly, while Palma et al. (2008) observed
106 a good coincidence of seismic and visual explosive activity, Goto and Johnson (2011) re-
107 ported a lack thereof. Thousands of repetitive events - denoted as LP events - were de-
108 tected by Richardson and Waite (2013) during 2010-2012 and later described as Strom-
109 bolian events (Richardson et al., 2014). We acknowledge that the terms “long-period event”
110 and especially “explosion” are used in the literature addressing Villarrica to describe the
111 transient waveforms. However, we think that usage of the term “explosion” insinuates
112 a knowledge about the nature of these events which in our view is not truly confirmed
113 at present. The descriptive term “long-period” on the other hand is inappropriate for
114 these waveforms if recorded close to the source since it commonly implies an upper fre-
115 quency limit around 5 Hz (Chouet, 1996). Therefore, and to be consistent with a pre-
116 vious publication by Lehr et al. (2019), we prefer the neutral term “transient”.

117 Volcano-tectonic events (VTs) are rather rare with 1-3 events per month reported
118 by Calder et al. (2004) for the years prior to 2004, and respectively to about 100 events

119 per week in early March 2012 (Mora-Stock (2015), this study). This difference however
 120 is probably the result of a different station set up rather than a true increase in the num-
 121 ber of VTs.

122 Studies by Witter et al. (2004); Mather et al. (2004); Palma et al. (2008); Guri-
 123 oli et al. (2008); Palma et al. (2011); Moussallam et al. (2016); Aiuppa et al. (2017) on
 124 gas flux rates, gas and magma composition indicate that vigorous convection of a two-
 125 phase system (gas bubbles in liquid magma) takes place in the conduit. Convective two-
 126 phase flow could also explain the notorious seismic and infrasonic unrest (Ripepe & Marchetti,
 127 2002). Between 2000 and 2011 the daily means of typical degassing rates of SO₂ at Vil-
 128 larrica ranged between 0.5 and 20 kg/s with an average at 5 kg/s and rarely exceeded 50 kg/s
 129 during periods of enhanced activity (Witter et al., 2004; Mather et al., 2004; Palma et
 130 al., 2008; Bredemeyer & Hansteen, 2014).

131 Two studies by Moussallam et al. (2016) and Liu et al. (2019) investigated peri-
 132 odicities in gas parameters at sampling rates of 0.125-1.0 Hz. Although both studies mea-
 133 sured the SO₂ flux at comparable locations of the plume (slightly above the crater rim
 134 and approximately 200 m above the magma surface (Moussallam et al., 2016)) Moussallam
 135 et al. (2016) showed periodicities at 30-380s while Liu et al. (2019) found cycles of 345-
 136 714s. However, Moussallam et al. (2016) themselves were reluctant about their findings,
 137 since contemporaneously measured gas concentration and temperature lacked any pe-
 138 riodicity. Interestingly, Liu et al. (2019) observed cycles on a similar scale (30-50 s) but
 139 in SO₂ concentration within the plume (using a drone). These differences are possibly
 140 caused by an exceptionally low SO₂ flux during Moussallam’s campaign. From the largely
 141 lacking periodicities Moussallam et al. (2016) deduced an efficient mixing of raising gas-
 142 rich and sinking degassed magma in the conduit resulting in a steady gas composition
 143 and flux rate. Liu et al. (2019) in contrast reported notable, audible bursts before the
 144 peaks in the SO₂ concentration. Moreover, they found a significant lack of correlation
 145 between the SO₂ concentration measured inside the plume directly above the crater and
 146 that measured by an instrument positioned approximately 100 m downwind at the crater
 147 rim. From the former finding, they concluded that the structure of the gas plume was
 148 predominantly formed by the (active) degassing process of the magma whereas from the
 149 latter, they inferred a nevertheless considerable influence of atmospheric effects (vari-
 150 able wind speed, turbulences, etc.). Due to a low CO₂/SO₂ molar ratio of around 1:1,
 151 they also suggested that gas bubbles remain coupled to the magma until reaching shal-
 152 low depths and being actively released. Periodicities on time scales of hours to weeks were
 153 reported in SO₂ degassing rates (Bredemeyer & Hansteen, 2014) as well as seismic am-
 154 plitude (Palma et al., 2008; Richardson et al., 2014)

155 **3 Renewal processes and interevent times in seismology and volcanol-**
 156 **ogy**

157

Period of Observa- tion	Activity	Cv	Distribution	Reference	Remarks
Stromboli Sept. 1997	SE	≈1	Exponential	Bottiglieri et al. (2005)	
May 2002 - Jan. 2003, Oct. 2006 - Mar. 2007, Sept. 2010 - May 2011	SE, Effusion	≈0.8	Exponential	Martino et al. (2012)	

158

continued on next page

continued from previous page						
Period of Observation	Activity	Cv	Distribution	Reference	Remarks	
29 April - 1 May 2005, 11-13 Jan. 2006, 20-22 Sept. 2007, 7-9 July 2008, 19-21 July 2009 1-31 July 2011	Intermittent SE Swarms	0.4-0.7	Other	Taddeucci et al. (2013)	Video analysis	
	SE		$Weibull(\lambda = 174 - 580, k = 0.87 - 1.20)$			
	Erebus Feb. 2005	SE	0.99	Exponential	De Lauro et al. (2009)	
		Feb.- April 2006	SE	26.73	Varley et al. (2006)	
Sept. 1984 - July 2004	Expls. related to bubble bursting in lava lake					period includes long periods of quiescence
Nov. 1999 - Mar. 2001	as above	1.36	$Log - logistic(\lambda = 0.026, k = 1.606, \tau_0 = 2.983)$		Subperiod of the above with continuous activity	
Etna 1-31 Aug. 2005			$Gamma(\lambda = 0.54, k = 1.83)$	Cauchie et al. (2015)	LPs, similar normalized distributions for Stromboli	
	1999-2005	Dyke intrusion	Deviance from tect. Scaling law	Traversa and Grasso (2010)	Vts	
Mt. St. Helens	degassing, Strombolian activity		Tectonic scaling law			
	dominant LP waveform		periodic	Matoza and Chouet (2010)	LPs	
Vesuvius 1972-2006	weaker LP waveforms		Exponential			
	fumaroles, moderate seismic activity		Tectonic scaling law	Traversa and Grasso (2010)	VT event	
Tungurahua July - Aug. 2004	explosions (impulsive waveforms)	2.9	$Log - logistic(\lambda = 0.135, k = 1.272)$	Varley et al. (2006)		
	degassing (emergent waveforms)	3.46	$Log - logistic(\lambda = 0.0721, k = 1.163)$			
	explosions+degassing	2.83	$Log - logistic(\lambda = 0.256, k = 1.501, \tau_0 = 0.288)$			
13-14 Juli 2013	24 h pre-eruptive drumbeat LP swarm	625	$Gamma(\lambda = 1, k = 2.256)$	Bell et al. (2018); Ignatieva et al. (2018)	LPs, only normalized distribution given	

continued on next page

159

continued from previous page					
Period of Observation	Activity	Cv	Distribution	Reference	Remarks
Volcan de Colima May 2002 - Sept. 2004	degassing (emergent waveforms), explosions (impulsive waveforms)	1.05-1.48	Log-logistic, Gamma, Weibull depending on event type and subperiod	Varley et al. (2006)	5 subperiods were analyzed
Karymsky 1997	SE	0.68	$Weibull(\lambda = 0.157, k = 1.234, \tau_0 = 1.009)$	Varley et al. (2006)	2 representative days
1998	SE	0.53	$Weibull(\lambda = 0.33, k = 1.393, \tau_0 = 1.0085)$		3 representative days

Table 1. Overview of studies addressing interevent times of volcanic seismicity. Parameters of probability density distributions were adapted to meet the definitions given in Table 2 if necessary. SE = Stromboilan explosion.

The occurrence of events in time is mathematically equivalent to points distributed on the positive real line, provided that their duration is negligible. Sequences of such events can be modeled stochastically by their interevent times, that is, the duration between two consecutive events. If these are independent and identically distributed the sequence is a renewal process. Renewal theory originated from queuing problems and failure time analysis in engineering and is part of the broader concept of point processes (Daley & Vere-Jones, 2003). The best-known and most fundamental renewal process is the Poisson process which has exponentially distributed interevent times. Poisson processes characterize completely random occurrence of events. For example, the global occurrence of large earthquakes or volcanic eruptions (la Cruz-Reyna, 1991) follows a Poisson process. In contrast, processes can be more clustered in time, e.g. as mainshock-aftershock sequences, or more periodically, in which case other distributions are used. For example, Bell et al. (2018) used a Gamma distribution to describe the quasi-periodic occurrence of repetitive long-period events before an eruption of Tungurahua.

In statistical seismology, the analysis of interevent times has gained new interest after the proposition of a universal scaling law by Bak et al. (2002) and Corral (2003). This scaling function is a Gamma distribution (Corral, 2003; Traversa & Grasso, 2010):

$$f(t) = Ct^{\gamma-1} \exp\left(\frac{-t}{a}\right) \tag{1}$$

with $\gamma = 0.67 \pm 0.05$, $a = 1.58 \pm 0.15$ and $C = 0.5 \pm 0.1$. When scaled by the corresponding rate, interevent time distributions of tectonic earthquake sequences from different regions collapse to Eq. 1. The theoretical foundation and the usefulness of Eq. 1 have been widely disputed, e.g. by Molchan (2005); Saichev and Sornette (2006); Touati et al. (2009). Nevertheless, on an empirical base, the scaling property and the fit to Eq. 1 have been demonstrated successfully for event catalogs across a wide range of scales such as acoustic emissions from fracturing rocks (Davidsen et al., 2007), induced seismicity at mining and drilling sites (Davidsen & Kwiatek, 2013), VT events (Bottiglieri et al., 2009; Traversa & Grasso, 2010) and regional tectonic events (Corral, 2003). Therefore,

187 we use it here as a reference to test whether a group of events behaves like shear frac-
188 tures.

189 Renewal processes were also used to model volcanic eruption sequences on differ-
190 ent scales. Repose intervals of indexed historic eruptions at numerous volcanoes have been
191 fitted by exponential, Gamma, Weibull and other distributions (see Marzocchi and Bebb-
192 ington (2012) for references). Notably, Dzierma and Wehrmann (2010) analyzed the
193 record of Villarrica Volcano and found the best fit for an exponential distribution (com-
194 pared to Weibull and Log-logistic). In analogy to earthquake statistics, Sanchez and Shcherbakov
195 (2012) derived a scaling function for major volcanic eruptions of 26 volcanoes, which is
196 a log-normal distribution. On a smaller scale, explosions, volcano-tectonic earthquakes,
197 long-period and very-long-period events - usually identified from geophysical monitor-
198 ing data - were analyzed for a number of volcanoes. A non-exhaustive overview stating
199 the type of events and, if provided, the distribution of interevent times, is given in Ta-
200 ble 1. In this list, the systems of Stromboli and Erebus are usually considered the most
201 similar to Villarrica as they are all basaltic open-vent systems. The majority of these
202 studies is based on seismological records. The analysis of interevent times using gas-related
203 measurements is rather uncommon. One exception was provided by Pering et al. (2015)
204 who used an SO₂ camera to detect gas bursts at Mt. Etna. They found a unimodal, skewed
205 left distribution with a median of about 5 s and a mode around 4 s.

206 4 Data

207 4.1 Seismic data

208 The seismic data were acquired during the installation of a dense local network com-
209 prising 75 seismometers during 1-12 March 2012 (Rabbel & Thorwart, 2019). Three sta-
210 tions were deployed at the crater rim (KRA1-KRA3) and the remaining instruments were
211 distributed on and around the volcanic edifice (Fig. 1). One of the crater stations (KRA2)
212 ceased to operate after 5 days whereas the other two (KRA1, KRA3) recorded for 12 days.
213 Due to their proximity to the active vent, they provided the most detailed recording of
214 its seismic activity. The stations were equipped with 3-component and 1-component SM-
215 6/U 4.5-Hz geophones, respectively, and DSS-cubes sampling at 100 Hz. We verified in
216 a laboratory experiment, that their data can reliably be recovered up to a tenth of the
217 nominal frequency (i.e. 0.45 Hz) by correcting for the instrument response.

218 The raw data were merged to 25-h-long sections and a constant trend removed. These
219 sections contained 24 h of data and additional 30 min at the beginning and end, which
220 overlapped with the previous and next sections. The data was filtered below 25 Hz and
221 resampled at 50 Hz. Subsequently, the instrument response was removed. Before the fi-
222 nal analysis, the overlap was sliced off to eliminate potential edge effects from filtering.

223 The seismic signal throughout the network was dominated by a persistent unrest
224 with overlain transient increases in amplitude which originated from the crater region
225 (Lehr et al., 2019). At the crater rim, these transients last from a few seconds to sev-
226 eral tens of seconds and contain frequencies up to 16 Hz. Fig. 2 shows a 6h-long record
227 section (top) and spectrograms and waveforms (middle) of the transient events as seen
228 by a near-source seismic station (KRA1) at the crater rim. The bottom panel includes
229 a similar transient signal at the distant station VS12. Note the substantial alteration of
230 the waveform with distance. We denote generally all the short-lived, more or less impul-
231 sive amplitude increases recorded at KRA1-3 as transients and refrain from any further
232 classification or attribution of source mechanisms.

233 Throughout the campaign, several hundreds of volcano-tectonic events (Fig. 2, bot-
234 tom) occurred about 5 km to the east of the summit (Mora-Stock, 2015) at depths be-
235 tween 1-5 km. Their frequency content is above 5 Hz; they have clear first arrivals, P-
236 and S-phases and last only for a few seconds. Their signal is easily detected at stations

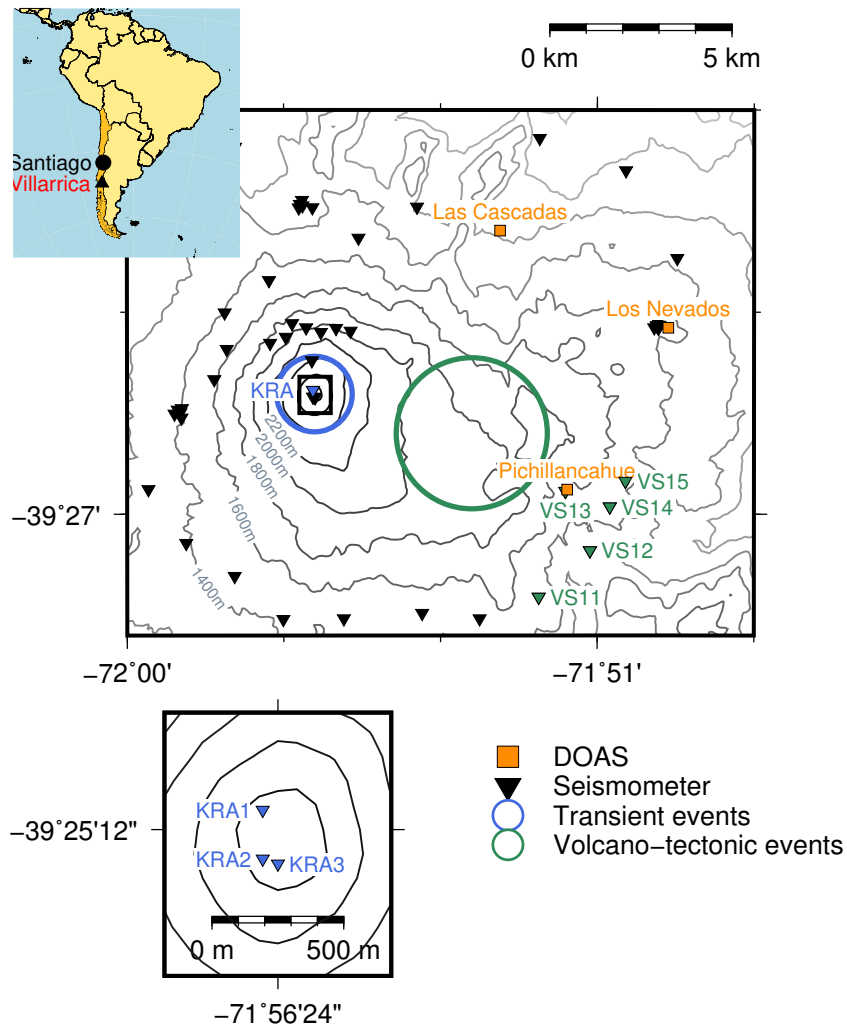


Figure 1. Locations of the three scanning Mini-DOAS stations (orange squares), 46 of the 75 deployed seismometers (black triangles), origins of transient and VT events (blue and green circles, respectively). Downwind distances of DOAS instruments from conduit center are (from N to S): Las Cascadas 6.76 km, Los Nevados 9.84 km, Pichillancahue 7.39 km. Seismometers used for the detection of transient and VT-events are colored in blue and green, respectively.

237 along the perimeter of the volcano but is masked by the volcanic noise at stations within
238 2-5 km to the crater and especially at the crater stations KRA1-3.

239 4.2 SO₂ flux

240 Differential optical absorption spectroscopy (DOAS) is a common technology to
241 measure e.g. the SO₂ content of a volcanic gas plume (Jochen Stutz, 2008; Platt et al.,
242 2018). In 2009 and 2010, three permanent scanning Mini-DOAS stations were deployed
243 around Villarrica Volcano at distances of about 7-10 km from the active crater in order
244 to continuously monitor its SO₂ emission rates (Fig. 1). For the present study we used
245 the data that was acquired during a 3-months period from 1 January to 31 March 2012
246 which generously covers the period of the seismic deployment. The NOVAC-type DOAS
247 instruments scan across the sky several kilometers downwind of the volcano and mea-
248 sure spectra of the incoming scattered sunlight in order to acquire SO₂ density profiles
249 of the volcanic gas plume vertically to its transport direction (Galle et al., 2010). By this
250 means the instruments intercept largely homogenized gas plumes, which are in thermal
251 equilibrium with the surrounding atmosphere. At wind speeds around 10 m/s the typ-
252 ical age of the plume is 10-15 min since emission from the vent. SO₂ slant column den-
253 sities at each scan angle were retrieved from the 310-320 nm wavelength range of the recorded
254 sunlight spectra by means of DOAS (Jochen Stutz, 2008). Additionally to the measured
255 sunlight spectra an SO₂ absorption spectrum from Vandaele et al. (1994), an O₃ absorp-
256 tion spectrum (Voigt et al., 2001), and a Ring spectrum to mitigate the Ring effect (Grainger
257 & Ring, 1962) were included in the DOAS fit. Plume transport velocities required to cal-
258 culate the flux from the SO₂ density profiles were estimated using archived wind speed
259 data of the National Oceanic and Atmospheric Administrations (NOAA) Global Fore-
260 cast System. Plume transport directions were determined by single station triangula-
261 tion using the SO₂ density profiles in combination with the best available information
262 on plume height. The latter either was determined by triangulation between the simul-
263 taneously acquired SO₂ density profiles of two DOAS instruments (Johansson et al., 2009),
264 or, if such simultaneous measurements were not available, the plume was assumed to be
265 stationary at the level of the emission source. The method requires UV-light, thus it only
266 works during daylight, and each scan through the gas plume takes 5-15 min depending
267 on the light conditions. This results in an irregularly spaced time series with gaps dur-
268 ing nighttime. The degassing rates of SO₂ varied between 0.14 and 80.91 kg/s at a mean
269 rate of 5.96 kg/s, a standard deviation of 5.7 kg/s and a median of 4.28 kg/s during the
270 study period.

271 5 Methods

272 At first, we directly compared the seismic amplitude with the degassing rate. Due
273 to the lack of visible correlation, we proceeded with the analysis of different seismic and
274 degassing events. The steps are explained in the subsequent subsections starting with
275 a recapitulation of the trigger algorithm and the definition of the different event types.
276 Based on the principle of the seismic trigger, we derived the idea of gas events. There-
277 after, the statistical methods are introduced to analyze the interevent times. Finally, us-
278 ing the resulting distributions of interevent times as input, a numerical model of a re-
279 newal process is proposed to couple the degassing and seismic activity.

280 5.1 Comparison of seismic amplitude and SO₂ flux

281 Frequency analysis indicated a concentration of the seismic energy at the crater rim
282 in two frequency ranges: 0.5-5 Hz and 7.5-10 Hz (Supporting figure S1). For these fre-
283 quency bands, as well as 0.5-24.9 Hz, the median of the absolute amplitude was computed
284 using windows of 40.96 s (2048 data points), overlapping by 50%. Similar to the well-
285 known RSAM, the result can be used as an indicator of the intensity of the seismic ac-

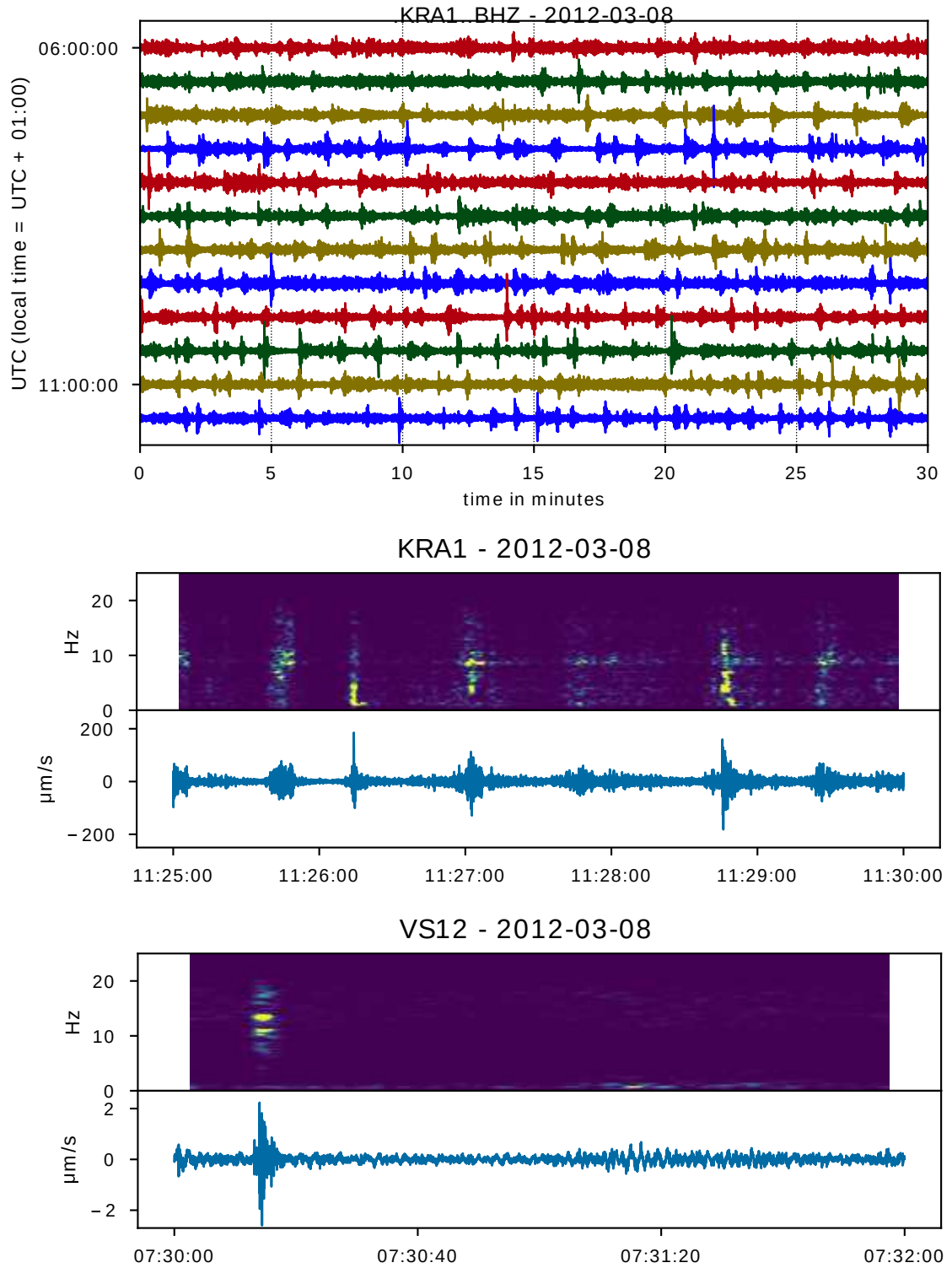


Figure 2. *top:* Seismicity recorded at the crater rim, $f=0.5\text{--}16\text{ Hz}$. We refer to the abundant, short-lived temporary increases in amplitude and spikes as “transient events”; *middle:* Spectrogram and detailed seismogram of transients at crater; *bottom:* Spectrogram and seismic trace of volcano-tectonic event (c. 07:30:10) and transient event (c. 07:31:10) 5 km SE of the crater.

286 tivity. The main difference is, that RSAM is based on the mean whereas here, we used
 287 the median because it is less sensitive to outliers. For comparison with the SO₂ flux the
 288 obtained amplitudes were smoothed again using a running median in windows of 1 h and
 289 24 h, respectively. The SO₂ flux data were averaged using the median of measured data
 290 points in consecutive 24 h- and 1 h-long time windows. Note however, that the 24 h-interval
 291 only includes data from during day light. The minimum and maximum in the respec-
 292 tive time windows indicate the variability of the flux.

293 5.2 Event detection

294 A simple and widely used method for the detection of seismic events is the ratio
 295 of short-term average to long-term average (STA/LTA). Two types of seismic events were
 296 investigated: the transient waveforms from the crater and the volcanic-tectonic earth-
 297 quakes originating southeast of the crater. Then the concept of the trigger was extended
 298 to derive a definition of SO₂ (or degassing) events.

299 For the STA/LTA trigger, the mean of the squared amplitude is computed in a short
 300 and a long time window. These are slid along the trace and a trigger function is obtained
 301 from the ratio of the two averages. A trigger is declared, when the trigger function ex-
 302 ceeds a predefined threshold and terminated when the function falls below a second, usu-
 303 ally lower, threshold. The window lengths and thresholds need to be adapted to the tar-
 304 geted events and depend on their duration, dominant frequency and the amount of back-
 305 ground noise. We implemented the trigger algorithm such that the ratio is evaluated at
 306 the common center of the STA and LTA windows. In a second variation, we applied the
 307 median instead of the mean of the squared amplitude.

308 Eventually we were interested in the distribution of interevent times. We found,
 309 that these were quite sensitive to the choice of the trigger method and its correspond-
 310 ing parameters. Therefore, we applied additional techniques to refine the catalog, de-
 311 pending on the type of events. We refer to a final collection of events obtained by a given
 312 procedure as catalog.

313 5.2.1 Transient events

314 For the detection of the transient events from the crater, the stations KRA1 and
 315 KRA3 were used and both stations needed to be triggered to declare an event (network
 316 coincidence trigger). The data were filtered between 0.45 and 16 Hz, owing to the broad
 317 variety of spectral content of these events. We tested combinations of STA windows of
 318 6, 8, 12 and 16 s and LTA windows of 16, 24, 32, 48 and 64 s. Combinations at which both
 319 windows would be of the same length were omitted. The trigger thresholds were set to
 320 1.25, 1.5 and 2 and the offset threshold was always fixed to 70% of the onset.

321 In order to evaluate the quality of the detection methods, we picked three 2-hour
 322 sequences manually. However the classification of a signal as event is to some degree sub-
 323 ject to interpretation. The success was quantified by the amount of correctly (n_{pos}) and
 324 falsely (n_{neg}) detected events compared to the number of reference event n_{ref} as

$$s = \sqrt{\left(1 - \frac{n_{pos}}{n_{ref}}\right)^2 + \left(\frac{n_{neg}}{n_{ref}}\right)^2} \quad (2)$$

325 Hence, the amount of missed and falsely detected events was minimized in a least-square
 326 sense. A successful detection was declared if a reference had an overlapping counterpart
 327 in the automatically generated catalog. A falsely detected event arose if no correspond-
 328 ing reference event could be found. In doing so, we ignored the differences regarding on-
 329 set times and duration between the automatically and manually detected events. Hence,
 330 we only tested whether the algorithm was capable of finding an event at all.

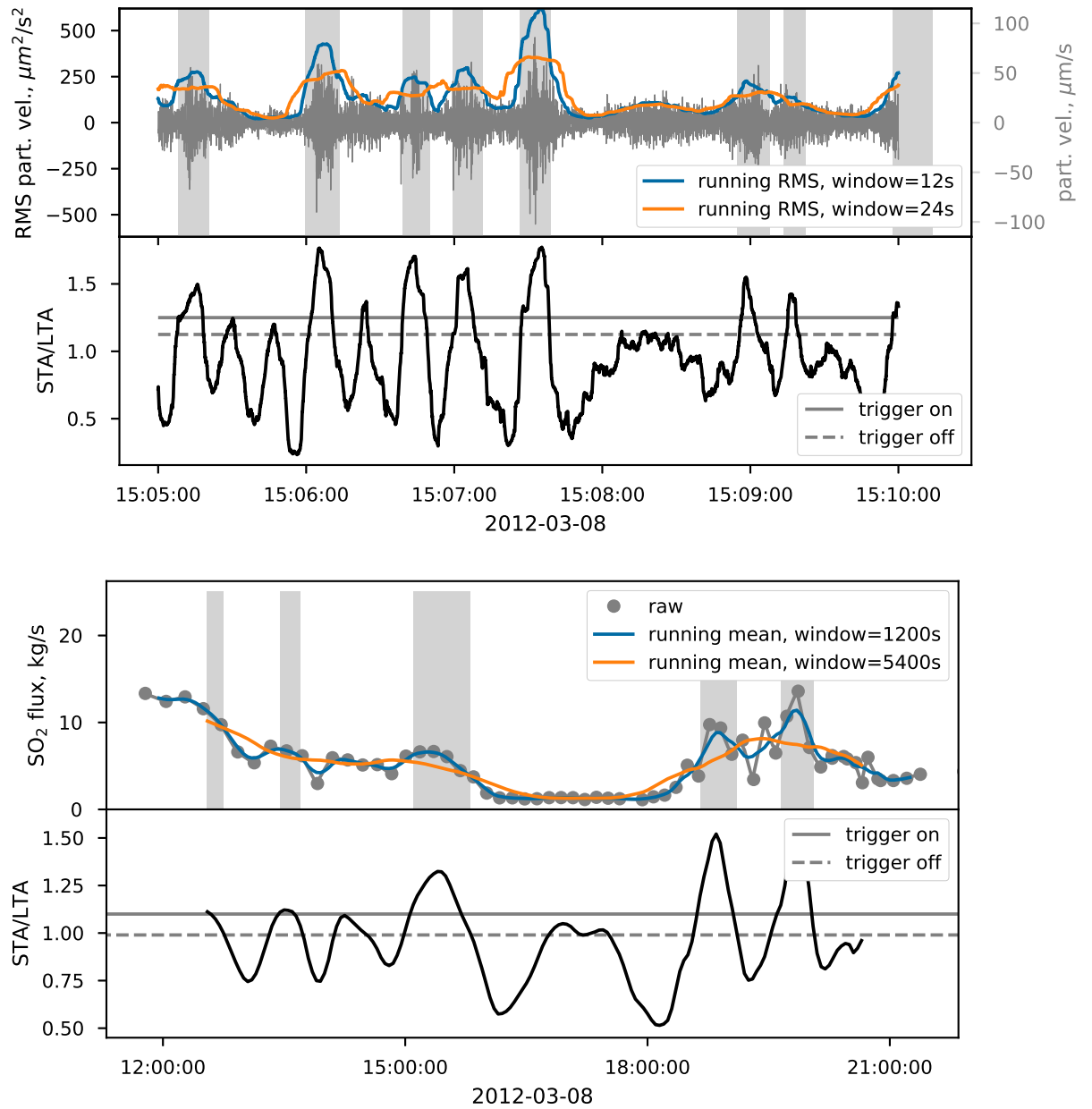


Figure 3. Event detection using an STA/LTA trigger on seismic (top) and gas (bottom) data: the trigger function (respective lower panels) results from the ratio between the average amplitude in a short (blue) and a long (red) window running in parallel. An event starts when the trigger function exceeds the “on”-threshold and terminates when the function drops below the “off”-threshold. For the seismic data the root-mean-square instead of the mean amplitude was used.

331 **5.2.2 VT-events**

332 For the detection of VT-events, we initially applied an STA/LTA trigger using the
 333 stations VS11-15 and filtering the data between 5 and 10 Hz. The catalogs were also quite
 334 influenced by the window lengths. However, due to the relatively low number of events
 335 it was feasible to revise the catalog manually. This included the removal of regional earth-
 336 quakes and quakes from parts of the edifice other than the main source region of VTs.
 337 Furthermore, several weak VTs were added.

338 **5.2.3 SO₂ events**

339 In analogy to seismic events, which are essentially local maxima in seismic ampli-
 340 tude, we determined SO₂ events by applying the STA/LTA trigger to the gas time se-
 341 ries. We experimented with window lengths of 10 min, 15 min, 20 min and 30 min for STA
 342 and 30 min, 45 min, 60 min, 90 min and 120 min for LTA. Thresholds were set to 1.01 and
 343 1.1. It should be noted that the original measurements were provided approximately ev-
 344 ery 10 min. The data were linearly interpolated to regular spaced 180 s-long intervals for
 345 gaps of less than 0.5 h and set to None otherwise. An example is shown in Fig. 3, bot-
 346 tom.

347 **5.3 Statistical aspects of interevent times**

348 We defined the interevent time as the time difference between two consecutive ar-
 349 rivals of events and analyzed their frequency distributions by computing histograms. In
 350 order to describe the overall shape of the distributions, we used the coefficient of vari-
 351 ation C_v which is defined as the mean divided by the standard variation of the interevent
 352 times. This term has been widely used in statistical seismology to differentiate between
 353 random processes ($C_v = 1$, exponential distribution of interevent times), periodic pro-
 354 cesses ($C_v < 1$) and processes clustered in time ($C_v > 1$, power-law distribution).

355 Since the three kinds of events occur on different time scales, we normalized the
 356 distributions by the respective means to compare their geometries. This procedure was
 357 inspired by the much debated, postulated scale invariance of the interevent times of tec-
 358 tonic earthquakes (see e.g. de Arcangelis et al. (2016) for a review).

359 Selected catalogs of each rescaled data set were modeled as common probability
 360 density distributions using the build-in maximum-likelihood estimation of `scipy.stats`. We
 361 tested for log-normal, exponential, log-logistic, Gamma and Weibull distributions (Ta-
 362 ble 2) and selected by the Akaike Information Criterion (AIC, Akaike (1974)).

363 **5.4 Renewal process model of coupled seismicity and degassing**

364 Furthermore, we developed a statistical model in which the occurrence of degassing
 365 events was derived from the occurrence of transients. The transients were modeled as
 366 a renewal process with interevent times drawn from a probability density distribution.
 367 We then assumed that the probability of a degassing event increases with the number
 368 of seismic events since the last degassing:

$$p(E_{SO_2} | n_{TRA}) = f(n_{TRA}) \quad (3)$$

369 A second series of degassing events was derived by testing for each transient whether
 370 it triggered a gas event. In other words, we performed a Bernoulli trial on each transient
 371 with the probability of success (=triggering) given by Eq. 3 and the current number of
 372 transients since the last degassing. A Bernoulli trial is a random experiment with only
 373 two outcomes, 0 or 1, that have probabilities q and p , respectively, with $q+p = 1$. The
 374 time of a gas event was defined as the time of the transient that triggered the degassing.
 375 This model was simulated numerically using Algorithm 1 for different $f(n_{TRA})$. Each

Name	Definition	
Exponential	$f(t; \lambda) = \frac{1}{\lambda} e^{-(t/\lambda)}$	$t, \lambda > 0$
Gamma	$f(t; \lambda, k) = \frac{1}{\Gamma(k)} \left(\frac{t}{\lambda}\right)^{k-1} e^{-\frac{t}{\lambda}}$	$t, \lambda, k > 0, \Gamma(k)$ -Gamma fct.
Weibull	$f(t; \lambda, k) = \frac{k}{\lambda} \left(\frac{t}{\lambda}\right)^{k-1} e^{-(t/\lambda)^k}$	$t, \lambda, k > 0$
Log-logistic	$f(t; \lambda, k) = \frac{(k/\lambda)(t/\lambda)^{k-1}}{(1+(t/\lambda)^k)^2}$	$t, \lambda, k > 0$
Log-normal	$f(t; \lambda, k) = \frac{1}{kt/\lambda\sqrt{2\pi}} \exp\left(-\frac{\ln^2(t/\lambda)}{2k^2}\right)$	$t, \lambda, k > 0$

Table 2. Parametrizations of the probability density functions used in this study. k and λ denote shape and scale parameters, respectively.

376 experiment was repeated 100 times using sequences of 20,000 transients. The interevent
 377 times of the transients were modeled according to the results from the observational data
 378 (a log-normal distribution). For f , we tested a step function (meaning E_{SO_2} happens
 379 after m transients), a constant probability and a linear and polynomial increase. The
 380 parameters for f were adapted by trial and error to match the observed data. From Eq. 3,
 381 another two interesting relations can be derived. The probability of an E_{SO_2} after the
 382 k -th transient since the last degassing is $P(E_{SO_2} \text{ after } k E_{TRA}) = \sum_{k=1}^N p(k)$ (corre-
 383 sponding to a cumulative distribution function). The probability at the k -th transient
 384 is given as the derivative.

Algorithm 1 Pseudocode for the coupled renewal processes of degassing and transient events. Curly brackets indicate comments

```

T_EXP = D()
n_EXP = 0 {counter for number of E_EXP after last E_SO2}
for t_i in T_EXP do
    p(E_SO2 | n_EXP) = f(n_EXP)
    if Bernoulli(p(E_SO2 | n_EXP)) = 1 then
        t_j,SO2 = t_i, {Triggering degassing event}
        n_EXP = 0 {Reset counter}
    else
        n_EXP += 1
    end if
end for
    
```

385 6 Results

386 6.1 Comparison of seismicity and SO₂ flux

387 A comparison of the seismic and SO₂ flux time series did not reveal any correla-
 388 tion (Fig. 4). On a long-term scale (top panel of Fig. 4), there was no accordance between
 389 the two data sets, even under the assumption of a time shift of several days. Such a shift
 390 might result from a delayed reaction of the seismicity to a change in the degassing regime
 391 or vice versa. On a more detailed scale (bottom panel of Fig. 4), single days and frequency
 392 ranges exhibited a seemingly good consistency between gas flux and 7.5-10 Hz- seismic
 393 amplitude, e.g. days 62, 65, 70 (Fig. 4). However, when taking into account all available
 394 days, the overall correlation was poor.

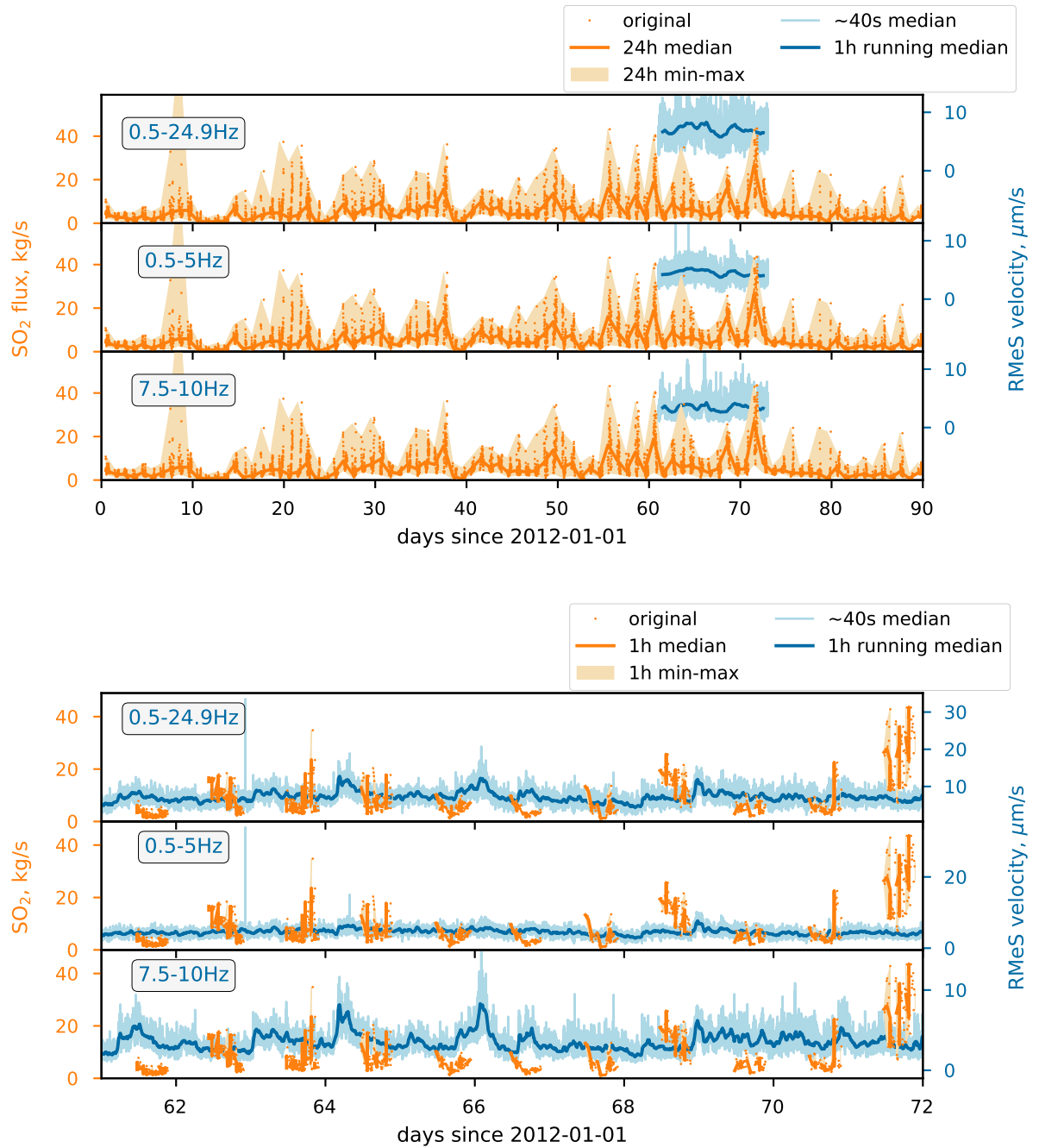


Figure 4. Comparison of SO_2 flux (orange, left) and seismicity at station KRA1 (blue, right) at different frequencies. SO_2 flux is given as median flux in consecutive 24h (top) and 1h (bottom) intervals and is identical in all panels. Seismicity is filtered as indicated and given as 24h and 1h running median of RMeS velocity in 20.48s windows at 5.12s intervals. There is only a poor correlation.

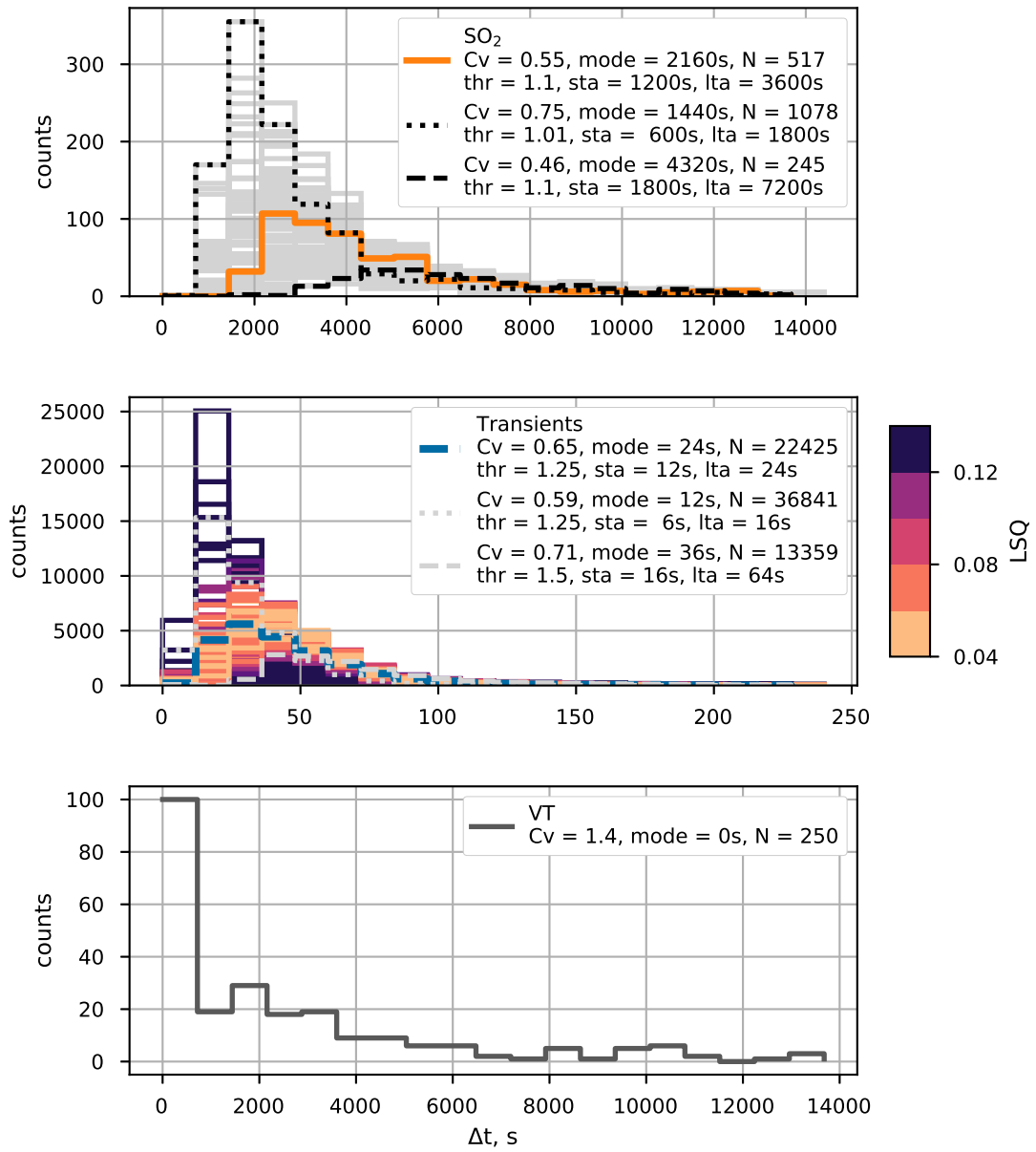


Figure 5. Distributions of interevent times for the three event types. SO_2 (top): All catalogs are shown in gray and two extremes are highlighted in black. The final selection is marked in orange. Transients (middle): Tested catalogs are color-coded by their success rate (Eq. 2) compared to manual picking. Low values/light colors indicate a high success. Two extreme cases are marked by dotted and dashed lines, respectively. The final selection is highlighted in blue. VT (bottom): Only data from the manually revised catalog is shown. Trigger parameters of highlighted catalogs and coefficient of variation (C_v), mode and total number of events (N) of corresponding distributions are given in the panels.

395

6.2 Interevent times

396

397

398

399

400

401

402

The empirical frequency distribution of the interevent times of all three event types (SO_2 , transients, VTs) was analyzed by histograms (Fig. 5). The results for the degassing and transient events depended substantially on the trigger parameters. Generally, distributions resulting from extreme parameter combinations formed the margins of the ensemble. Only results for which the amplitudes in the STA and LTA windows were averaged by the mean are presented here. Separate plots of each catalog, including the results for median averaging are provided in the supporting information (Figs. S2-4).

403

404

405

406

407

408

409

410

411

For all catalogs of transient events, the histograms of interevent times indicated skewed right, unimodal distributions while the number of detections ranged roughly from 10,000 to 50,000. The coefficient of variation C_v increased with threshold and varied between 0.4 and 2, thus giving no clear indication of the type of process. However, C_v for catalogs, that yielded a quality of 0.06 or better, fell between 0.4 and 0.7 which consistently indicated a rather periodic process. The best correspondence between an automatically generated catalog and the manual picks was achieved for mean/threshold=1.25/STA=12 s/LTA=24 s with $s=0.042$. The mode of this distribution lay between 20 s and 25 s. For distributions of similar quality ($s<0.06$), the mode was located between 20 s and 30 s.

412

413

414

415

416

417

418

419

420

421

422

423

Similarly to the transient events, the histograms for the gas events indicated generally skewed right, unimodal distributions. The number of detected events ranged between 78 and 596 with a mode around 1 h. C_v varied between 0.43 and 0.77, which indicated a periodic process irrespective of the trigger settings. Except for STA=0.17 h (20 min) and STA=0.25 h (15 min) in combination with LTA=0.75 h and a threshold of 1.1, the trigger settings yielded largely similar numbers of detected events, coefficients of variations and shapes of histograms. Regarding STA=600 s, one should bear in mind that this interval contained effectively only 1-2 real data points. Thus these catalogs were potentially strongly influenced by outliers in the data. Nevertheless, the resulting distributions were more or less identical to those obtained using longer STA windows. For further analysis, we chose the catalog mean averaging/threshold=1.1/STA=1200 s/LTA=3600 since it lies at center of the ensemble.

424

425

426

The histogram of the VT interevent times yielded a strongly skewed-right, unimodal distribution. The $C_v = 1.4$ indicated an exponential or power-law decay of interevent times. The number of detected events was 250 with a mean interevent time of 3096 s.

427

428

429

430

431

432

433

434

We fitted different probability density functions to the interevent times of the final catalogs, normalized by their respective mean (Fig. 6). The best model was selected by the lowest AIC. The interevent times of transients and degassing events were best represented by a log-normal distribution, while those of the VT events could be equally well fitted by a Gamma or Weibull distribution. For the VT events, we also tried an exponential distribution, but found the fit to be substantially lower than for the distributions shown here. Parameters of the best-fitting models are indicated in Fig. 7 (for parameters of other distributions see Table 1 in the Supplements).

435

436

437

438

439

440

441

442

443

The distributions of both, the transient events from the crater and the gas events exhibited a very similar pattern with respect to the trigger settings, albeit on very different time scales. Similarly, the coefficients of variation of the interevent times indicated a periodic process for both types of events. In contrast, the interevent times of the VTs indicated random occurrence or occurrences clustered in time. The best-fitting probability density functions of crater and gas events were strikingly similar, especially in comparison to the VT events (Fig. 7). It should be noted however, that the two-sample Kolmogorow-Smirnow-Test which tests whether two samples come from the same distribution did not indicate similarity within a reasonable confidence level.

444

445

The Gamma distribution of the volcano-tectonic interevent times resembled the tectonic scaling function (Eq. 1) even though the parameters were not identical (Fig. 7). In

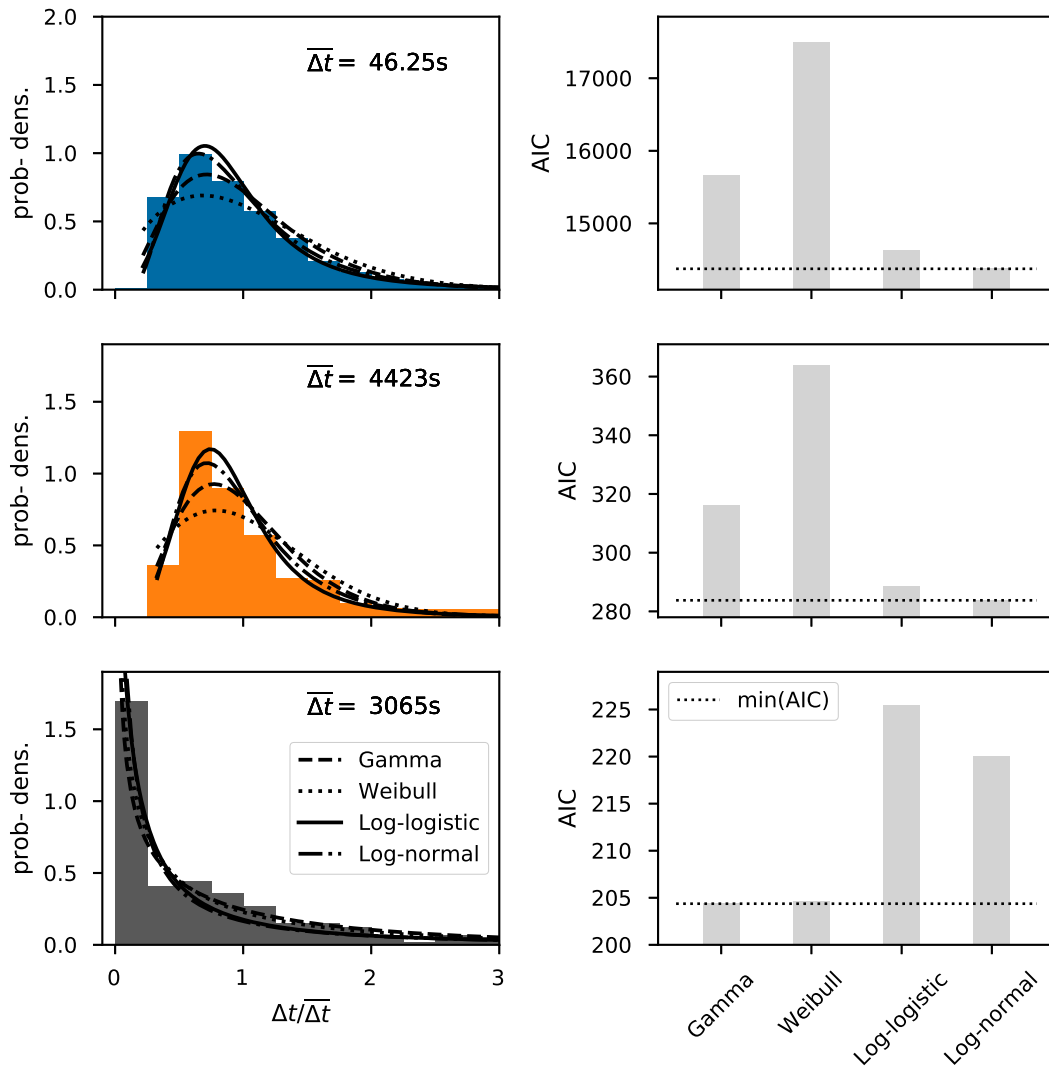


Figure 6. Left column shows histograms of interevent times, rescaled by the mean and different fitted probability distributions for transients (top row), gas (middle) and VT events (bottom). Right column shows values of Akaike Information Criterion for each distribution. Lower AIC indicates better relative fit.

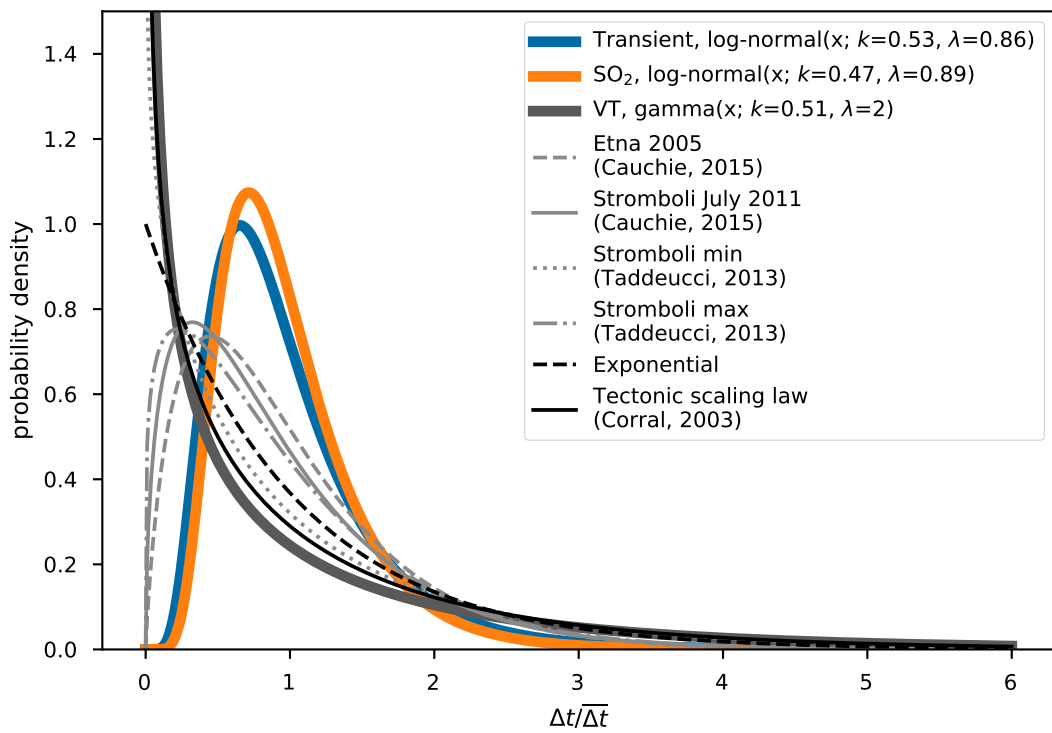


Figure 7. Rescaled interevent time distributions of transients, gas and VT events in comparison to other volcanoes. Interevent times are normalized by the respective mean. Distributions from literature are given in standardized form.

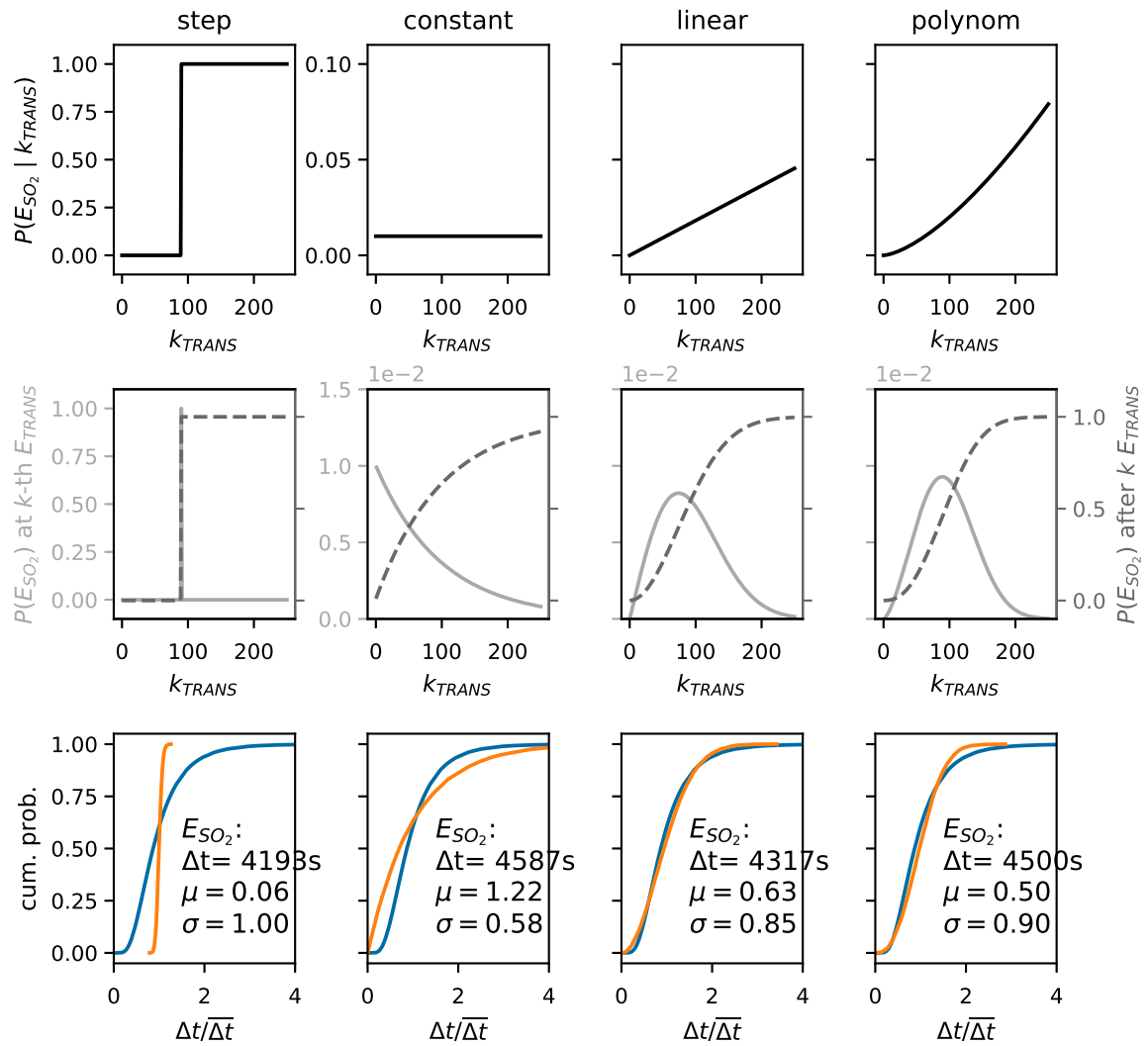


Figure 8. Coupled transient and degassing events as renewal process. *top row:* $p(E_{SO_2} | n_{TRA})$; *middle:* derived probabilities of degassing events at (solid, light gray lines) and after (dashed, dark gray lines) the k -th seismic transient since the last degassing; *bottom:* cumulative empirical distribution functions (EDF) of the rescaled interevent times of transients (blue) and degassing (orange). Columns correspond to the different scenarios of $p(E_{SO_2} | n_{TRA})$

446 contrast, the transient and degassing events had little in common with the distributions
 447 found for long-period or explosive seismicity at other volcanoes, especially not with the
 448 frequently encountered exponential distribution.

449 **6.3 Statistical modeling**

450 The log-normal distribution of the interevent times of transients was used in the
 451 proposed statistical model (Algorithm 1) to generate artificial sequences of events. The
 452 parameters of the different functions for $p(E_{SO_2} | n_{TRA})$ were adjusted manually to achieve
 453 a good agreement between the distributions of rescaled interevent times of transients and
 454 degassing. Fig. 8 summarizes the inputs and results. In the first scenario (step function),

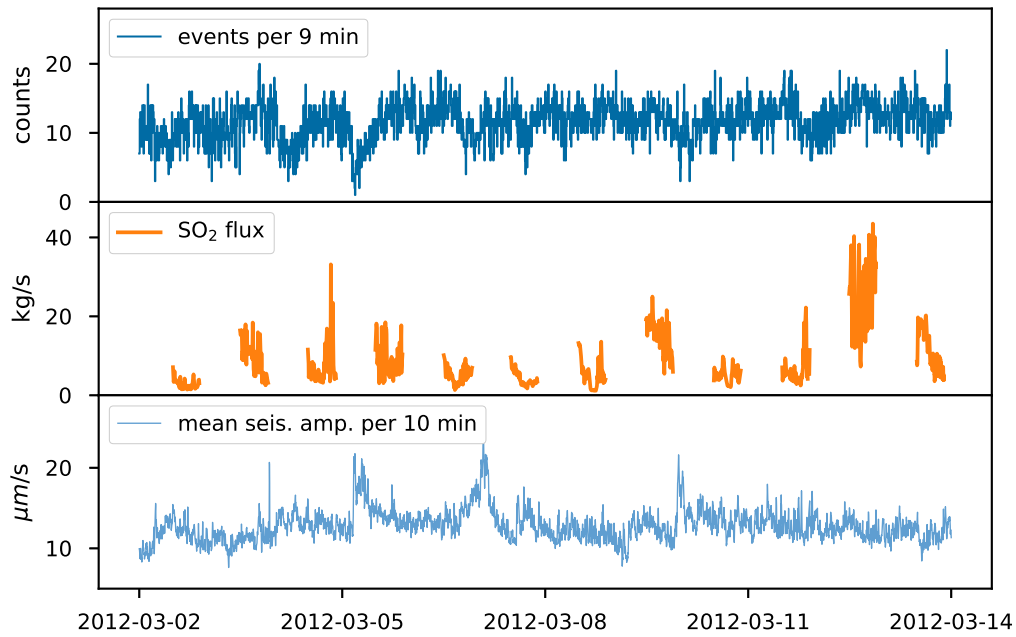


Figure 9. Time series of transients per consecutive 9-min interval, SO₂ flux and mean seismic amplitude in 10-min intervals, shifted by 3 min. Neither the seismic amplitude nor the amount of events per time correlate well with the degassing rate. Note, that the SO₂ flux is interpolated from irregular, approximately 10-min intervals to regular 3-min intervals.

455 a gas event simply occurs after a fixed number of transients. Obviously, it failed to re-
 456 produce the targeted empirical distribution function (EDF). The second scenario - each
 457 transient triggers degassing with the same probability - also failed to reproduce an im-
 458 portant feature of the targeted distribution, namely the inflection point. This was only
 459 achieved for an at least linear increase of the probability with the number of transients.
 460 Higher orders of increase then allowed an even finer tuning of the resulting EDF and a
 461 better match between the modeled and observed distributions.

462 In the model we assumed that the seismic signals are directly related to degassing
 463 activity. This gave rise to a new view on the correlation between the time series of de-
 464 gassing and seismicity: Instead of the amplitude, the number of events per time might
 465 correlate with the SO₂ flux. However, the number of events per unit time clearly shows
 466 the same lack of correlation with the gas flux as the amplitude. (Fig. 9).

467 7 Discussion

468 7.1 Event detection and catalog completeness

469 The extreme variety of seismic waveforms resulting from the transients complicated
 470 the identification and detection of these events. Therefore, the transient catalog is al-
 471 most certainly incomplete. In particular, events below the noise level can not be cap-
 472 tured by the STA/LTA trigger. We considered the approach of Cauchie et al. (2015) who
 473 used template matching to detect weak events and improve their catalog. Unfortunately,
 474 this was impractical for our data set due to the huge number of different waveforms. For
 475 the same reason, a machine learning algorithm based on hidden Markov models (Hammer
 476 et al., 2012) failed. Bell et al. (2017) used manual picking to compile their catalog, which

477 was firstly infeasible for our number of events and secondly limits the objectivity of the
478 detection method. Nevertheless, we revised the VT catalog manually, but used a fixed
479 set of rules to select the events which could have been implemented in the trigger algo-
480 rithm. We explored the uncertainty of the transient and SO₂ catalogs and its influence
481 on the interevent time statistics by testing various combinations of trigger parameters.
482 Despite the considerable differences, the various catalogs share one important charac-
483 teristic, namely a periodic rather than random occurrence of events.

484 7.2 Scale Invariance

485 The rescaled distributions of interevent times of degassing and transients are sur-
486 prisingly similar. Assuming, this similarity is real, the two observations could be the man-
487 ifestations of a self-similar/scale-invariant process on different time scales. A possible link
488 between them was demonstrated in the statistical experiment. However, it should be noted,
489 that log-normal distributions are frequently found in natural processes and the osten-
490 sible similarity might be purely incidental.

491 7.3 Interpretation as renewal process

492 In our statistical experiment, we explored a possible relationship between seismic-
493 ity and degassing based on very few, simple assumptions: the degassing activity is com-
494 pletely represented by the discrete seismic transients, and the probability of generating
495 a gas peak depends solely on the number of transients since the last degassing event. Within
496 this framework, we could show that, in order to meet the empirical observation, the prob-
497 ability of a degassing event needs to increase at least linearly with the number of seis-
498 mic events.

499 7.4 Seismicity as representative of active degassing

500 As a consequence of the discretization, we neglected a possibly important part of
501 information. In particular, the nature of the notorious seismic unrest at Villarrica is not
502 well understood. While some parts of it are certainly codas from single events (Richardson
503 & Waite, 2013) interfering with each other and the normal background noise, others might
504 be produced actively by continuous degassing processes and the convection of magma
505 in the conduit (Palma et al., 2008; Ripepe et al., 2010). Fluid migration is known to cause
506 sustained reverberations either in the magma column itself or of the conduit walls, which
507 is observable as LP events or tremors (Chouet, 1996). Especially the latter were not tar-
508 geted by the event detection. Similarly to the seismic unrest, the gas flux is continuous
509 and the detected events should be regarded as variations, possibly superposed on a back-
510 ground level.

511 We proposed a possible link between degassing and seismicity, expressed as a prob-
512 abilistic model. However the model does not indicate where or when the transition be-
513 tween the short time scales of the transient events and the longer times of the degassing
514 variation takes place. The transients form the base of our model but unfortunately, their
515 nature and origin is not very clear. Some authors generally describe the signals as ex-
516 plosions (Ortiz et al., 2003; Calder et al., 2004). Palma et al. (2008) claimed a good ac-
517 cordance with visible degassing processes at the surface of the lava lake (bubble burst-
518 ing etc.). Goto and Johnson (2011) on the other hand reported a lack thereof, which in-
519 dicates that these signals might also originate from deeper in the conduit. This would
520 be more consistent with the results of Richardson and Waite (2013) who interpreted the
521 moment tensor of a repetitive version of these waveforms as drag forces acting on the
522 lava lake bottom.

523 We suggest two alternative concepts, what the nature of the transients implies for
524 the degassing, illustrated in Fig. 10. If the signals originated solely at the free surface of

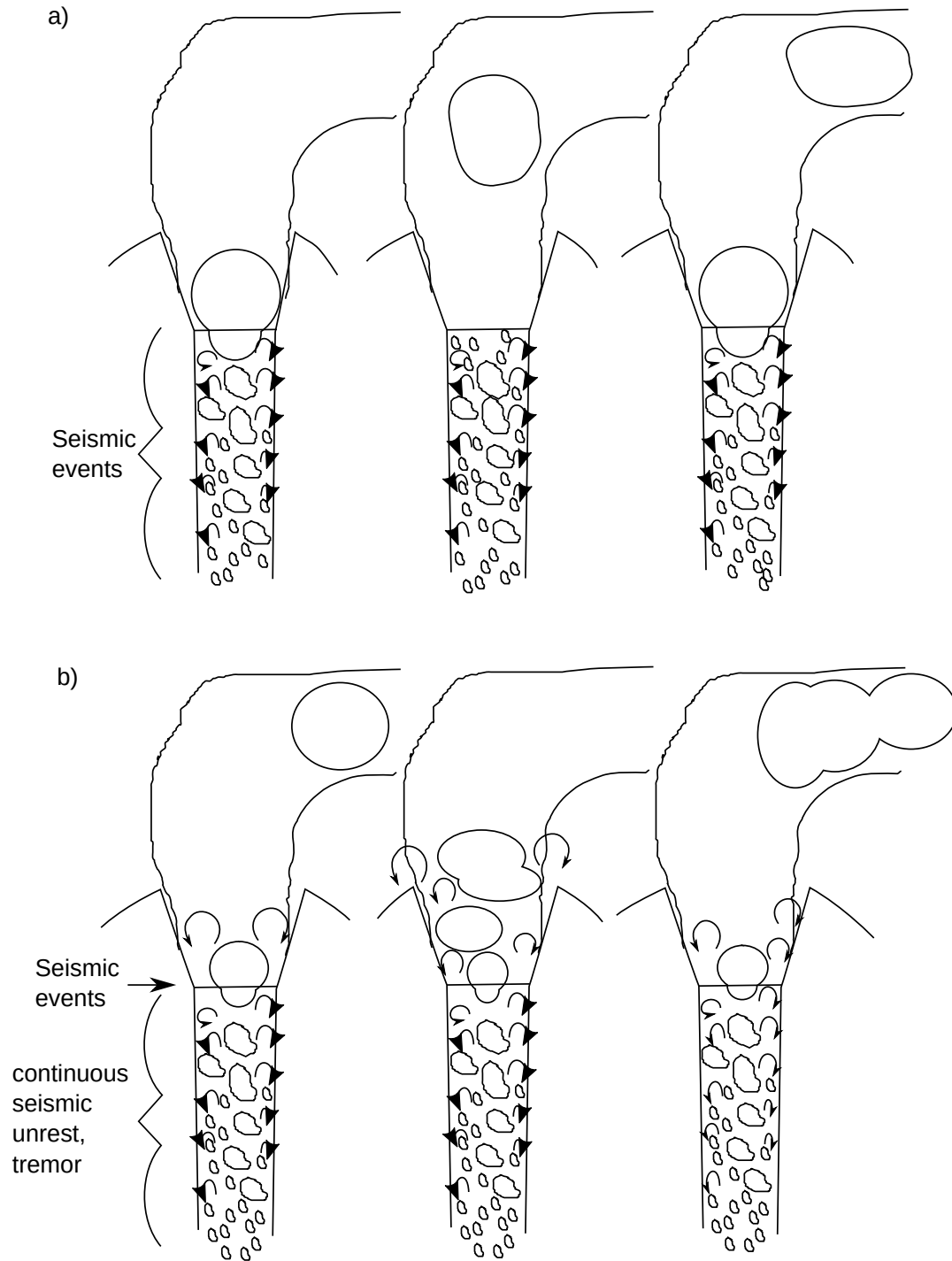


Figure 10. Two scenarios of where the transition between the time scales of the seismic events and the fluctuations of the degassing rate might occur: a) Seismic events originate from the whole conduit while gas accumulates into a slug that is released to form a temporary peak in the gas flux. b) Seismic events are produced solely by vigorous degassing (bubble/slug bursting) at the surface of the lava lake and gas fluctuations result from atmospheric mixing in the convectively rising portion of the plume.

525 the lava lake (Model B) each event would indicate a new release of gas to the plume. In
526 this case the transition between the time scales must be a result of mixing processes in
527 the atmosphere and plume dynamics. If however transients could also be produced at
528 some depth (Model A), the same gas unit (slug, bubble) could cause several seismic events
529 during its ascent through the conduit. Then, the transition would rather be a result of
530 the degassing and transport of the magma, even though additional atmospheric processes
531 can not be ruled out.

532 In both cases we assume that the seismicity is predominantly an expression of the
533 magmatic degassing. In any case the gas needs to accumulate somewhere to form the
534 observed long-term fluctuations unless we assume varying supply of gas at depth as a
535 third option. In principle, more gas could mean either more or bigger events. In the for-
536 mer case the number of events should be consistent with the gas flux while in the lat-
537 ter case it should be the seismic amplitude. However, neither is the case, which is why
538 we discarded this third option.

539 The results of Liu et al. (2019) support Model B for two reasons: 1) It revealed pe-
540 riods of 30-50 s - comparable to the mean interevent times of the transients - in close prox-
541 imity to the lake surface. This could be seen as indication that bubble bursts occur at
542 this rate at the surface and our transients may be the seismic expression of that. 2) They
543 report a significant difference to the periodicity recorded by the only slightly more dis-
544 tant station at the crater rim which they explain by atmospheric turbulences (suppl. Fig.S5).
545 In contrast, our DOAS instrument measured the plume several kilometers away from the
546 vent, leaving plenty of time and space for reorganization and homogenization of the ju-
547 venile plume and overprinting of early periodicities due to discrete gas releases. How-
548 ever, we can not exclude a deeper origin of at least some of the seismic events, which should
549 be the case for Model A.

550 **7.5 Comparison to other volcanoes and earthquakes**

551 The enigmatic nature of the transient events only allows for limited comparison with
552 other studies. These usually address a very specific volcanic activity (e.g. Vulcanian/Strombolian
553 explosions) and it is unclear, whether other activity and smaller events were not present
554 or were excluded from the analysis.

555 Erebus, similar to Villarrica, possesses an active lava lake. Varley et al. (2006) stud-
556 ied explosions related to bubble bursting in the lake, which occurred clustered in time.
557 Their period of observation was several months compared to our merely two weeks. Vil-
558 larrica was quite active during this time. Including periods of less activity might result
559 in a more clustered occurrence.

560 Palma et al. (2008) suggested that discrete bubble bursting at Villarricas lava lake
561 forms a continuum with Strombolian explosions. The latter, in their well-known form
562 as spectacular, meters high ejections of magma, are rare at Villarrica. Less impressive
563 bubble bursting however seems to be a plausible cause for the transients and therefore
564 their occurrence may be comparable to that of Strombolian explosions. At Erebus and
565 Stromboli, these were found to generally occur at random, resulting in an exponential
566 distribution of their interevent times (Table 1). Our study revealed a clearly periodic oc-
567 currence of the transient events. To our knowledge, this has been reported only for short
568 periods of high, unusual activity at other volcanoes. Assuming that Villarrica behaves
569 in a similar way and that the transient events are comparable to Strombolian explosions,
570 the log-normally distributed interevent times found in this study would indicate a pe-
571 riod of unusual activity. Indeed, the volcano was observed to be relatively active dur-
572 ing that time, producing several small ash eruptions and mild Strombolian activity (Fig.S6)
573 in March 2012 (Global Volcanism Program, 2014).

574 One of the most striking results is the clear difference between the rescaled interevent
575 times of transients and VTs. VTs generally seem to obey the same Gamma-distribution
576 as normal tectonic earthquakes. The only exception was reported by Traversa and Grasso
577 (2010) for Etna, where the interevent time distribution significantly changed during two
578 dyke intrusions. The VTs at Villarrica behave more or less as expected from the scal-
579 ing law. The deviation in the parameters of the Gamma distribution might be related
580 to the relatively low number of earthquakes in the catalog and false or missed detections.
581 Alternatively, it could be the result of a magma intrusion similar to the case at Etna.

582 7.6 Further remarks

583 A more detailed picture might arise if amplitudes were included in the model. Nev-
584 ertheless, we think, that this simplistic renewal process model provides an interesting new
585 aspect on the relation between degassing processes and seismic activity at volcanoes. More-
586 over, variations on much larger (days, months) or smaller (minutes, seconds) time scales
587 are possible but were not investigated here. Finally, it should be noted that the our seis-
588 mic observations covered a much shorter period than the gas data and that we extrap-
589 olated the statistical results to the remaining period of gas observations. We think this
590 is justified because OVDAS reported unchanging numbers of detected VTs and transients
591 (LPs in their terminology) for January-April 2012.

592 8 Conclusions

593 We found periodic recurrences of seismic transients and peaks in the SO₂ flux rate
594 at Villarrica volcano based on the coefficient of variation of the interevent times. The
595 modes of the distribution were at 24s for the transients and 2160s for the degassing events.
596 In contrast, volcano-tectonic events showed the time-clustered occurrence expected for
597 shear fractures with a mode at 0s and a mean interevent time of 3065s. The normal-
598 ized distribution functions of interevent times between transients and degassing events
599 are remarkably similar, even though the events occurred on very different time scales.
600 Provided seismic events and variations in SO₂ flux are part of the same process, this sug-
601 gests some sort of scale-invariance or self-similarity of the underlying time distributions.
602 In regard to the general lack of convincing correlations between seismic amplitude and
603 degassing rates, we suggest the analysis of interevent times as an interesting alternative
604 way to link degassing and seismicity. The proposed renewal model reproduces the em-
605 pirical observation very well, although it can not explain where the transition between
606 the two time scales physically happens. In that respect, the nature of the seismic events
607 requires more investigation. Simultaneous visual observations of the activity at the lake
608 surface and measurements at higher time-resolution and closer to the conduit of the gas
609 flux could further elucidate their role in the degassing process. Still, the discovered em-
610 pirical statistical distributions and model provide a benchmark that future physical mod-
611 els of the degassing process need to meet.

612 Acknowledgments

613 The seismic campaign was funded by the Deutsche Forschungsgemeinschaft Collabora-
614 tive Research Center CRC574. The seismometers were provided by the Geophysical In-
615 strument Pool Potsdam (GIPP) of the Deutsches Geoforschungszentrum Potsdam (GFZ).
616 The data are available through the GFZ Data Services (<http://doi.org/10.5880/GIPP.201202.1>).
617 The SO₂ flux data as well as the event catalogs are provided as Supporting Material. Data
618 analysis and visualization was realized by means of Python (notably Obspy, Numpy, Scipy,
619 Matplotlib, and Jupyter) and Generic Mapping Tools (GMT). We thank the numerous
620 developers for providing of these APIs.

References

- 621
- 622 Aiuppa, A., Bitetto, M., Francofonte, V., Velasquez, G., Parra, C. B., Giudice, G.,
623 ... Curtis, A. (2017, June). A CO₂ -gas precursor to the march 2015 villarrica
624 volcano eruption. *Geochemistry, Geophysics, Geosystems*, 18(6), 2120–2132.
625 doi: 10.1002/2017gc006892
- 626 Akaike, H. (1974, December). A new look at the statistical model identification.
627 *IEEE Transactions on Automatic Control*, 19(6), 716–723. doi: 10.1109/tac
628 .1974.1100705
- 629 Bak, P., Christensen, K., Danon, L., & Scanlon, T. (2002, April). Unified scaling law
630 for earthquakes. *Phys. Rev. Lett.*, 88, 178501. Retrieved from [https://link](https://link.aps.org/doi/10.1103/PhysRevLett.88.178501)
631 [.aps.org/doi/10.1103/PhysRevLett.88.178501](https://link.aps.org/doi/10.1103/PhysRevLett.88.178501) doi: 10.1103/PhysRevLett
632 .88.178501
- 633 Bell, A. F., Hernandez, S., Gaunt, H. E., Mothes, P., Ruiz, M., Sierra, D., &
634 Aguaiza, S. (2017, October). The rise and fall of periodic drumbeat seis-
635 micity at Tungurahua volcano, Ecuador. *Earth and Planetary Science Letters*,
636 475, 58–70. Retrieved 2018-04-19, from [http://www.sciencedirect.com/](http://www.sciencedirect.com/science/article/pii/S0012821X17304144)
637 [science/article/pii/S0012821X17304144](http://www.sciencedirect.com/science/article/pii/S0012821X17304144) doi: 10.1016/j.epsl.2017.07.030
- 638 Bell, A. F., Mark, N., Stephen, H., Main, I. G., Gaunt, H. E., Patricia, M., &
639 Mario, R. (2018, February). Volcanic Eruption Forecasts From Accel-
640 erating Rates of Drumbeat Long-Period Earthquakes. *Geophysical Re-*
641 *search Letters*, 45(3), 1339–1348. Retrieved 2018-04-19, from [https://](https://agupubs.onlinelibrary.wiley.com/doi/abs/10.1002/2017GL076429)
642 agupubs.onlinelibrary.wiley.com/doi/abs/10.1002/2017GL076429 doi:
643 <https://doi.org/10.1002/2017GL076429>
- 644 Bottiglieri, M., Godano, C., & D’Auria, L. (2009, October). Distribution of volcanic
645 earthquake recurrence intervals. *Journal of Geophysical Research: Solid Earth*,
646 114(B10), B10309. Retrieved 2018-02-13, from [http://onlinelibrary.wiley](http://onlinelibrary.wiley.com/doi/10.1029/2008JB005942/abstract)
647 [.com/doi/10.1029/2008JB005942/abstract](http://onlinelibrary.wiley.com/doi/10.1029/2008JB005942/abstract) doi: 10.1029/2008JB005942
- 648 Bottiglieri, M., Martino, S. D., Falanga, M., Godano, C., & Palo, M. (2005, Novem-
649 ber). Statistics of inter-time of Strombolian explosion-quakes. *Europhysics Let-*
650 *ters (EPL)*, 72(3), 493–498. doi: 10.1209/epl/i2005-10258-0
- 651 Bredemeyer, S., & Hansteen, T. H. (2014). Synchronous degassing patterns of
652 the neighbouring volcanoes Llaima, and Villarrica in south-central Chile: the
653 influence of tidal, forces. *International Journal of Earth Sciences*, 103(7),
654 1999–2012. Retrieved from <http://dx.doi.org/10.1007/s00531-014-1029-2>
655 doi: 10.1007/s00531-014-1029-2
- 656 Calder, E. S., Harris, A. J. L., Peña, P., Pilger, E., Flynn, L. P., Fuentealba, G.,
657 & Moreno, H. (2004). Combined thermal and seismic analysis of the vil-
658 larrica volcano lava lake, Chile. *Revista geológica de Chile*, 31(2), 259–
659 272. Retrieved from [http://www.scielo.cl/scielo.php?pid=S0716](http://www.scielo.cl/scielo.php?pid=S0716-02082004000200005&script=sci_arttext)
660 [-02082004000200005&script=sci_arttext](http://www.scielo.cl/scielo.php?pid=S0716-02082004000200005&script=sci_arttext) doi: [http://dx.doi.org/10.4067/](http://dx.doi.org/10.4067/S0716-02082004000200005)
661 [S0716-02082004000200005](http://dx.doi.org/10.4067/S0716-02082004000200005)
- 662 Cauchie, L., Saccorotti, G., & Bean, C. J. (2015, September). Amplitude and recur-
663 rence time analysis of LP activity at Mount Etna, Italy. *Journal of Geophysi-*
664 *cal Research: Solid Earth*, 120(9), 2015JB011897. Retrieved 2017-09-29, from
665 <http://onlinelibrary.wiley.com/doi/10.1002/2015JB011897/abstract>
666 doi: 10.1002/2015JB011897
- 667 Chouet, B. (1996). Long-period volcano seismicity: its source and use in eruption
668 forecasting. *Nature*, 380(6572), 309–316.
- 669 Corral, A. (2003, September). Local distributions and rate fluctuations in a uni-
670 fied scaling law for earthquakes. *Phys. Rev. E*, 68, 035102. Retrieved
671 from <https://link.aps.org/doi/10.1103/PhysRevE.68.035102> doi:
672 10.1103/PhysRevE.68.035102
- 673 Daley, D. J., & Vere-Jones, D. (2003). *An introduction to the theory of point pro-*
674 *cesses*. Springer-Verlag. Retrieved from [https://www.springer.com/de/](https://www.springer.com/de/book/9780387955414)
675 [book/9780387955414](https://www.springer.com/de/book/9780387955414) doi: 10.1007/b97277

- 676 Davidsen, J., & Kwiatek, G. (2013, February). Earthquake interevent time distri-
677 bution for induced micro-, nano-, and picoseismicity. *Physical Review Letters*,
678 *110*(6). doi: 10.1103/physrevlett.110.068501
- 679 Davidsen, J., Stanchits, S., & Dresen, G. (2007, March). Scaling and universality
680 in rock fracture. *Physical Review Letters*, *98*(12). doi: 10.1103/physrevlett.98
681 .125502
- 682 de Arcangelis, L., Godano, C., Grasso, J. R., & Lippiello, E. (2016, April). Statis-
683 tical physics approach to earthquake occurrence and forecasting. *Physics Re-*
684 *ports*, *628*, 1–91. doi: 10.1016/j.physrep.2016.03.002
- 685 De Lauro, E., De Martino, S., Falanga, M., & Palo, M. (2009, October). Modelling
686 the macroscopic behavior of Strombolian explosions at Erebus volcano. *Physics*
687 *of the Earth and Planetary Interiors*, *176*(3-4), 174–186. doi: https://doi.org/
688 10.1016/j.pepi.2009.05.003
- 689 Dzierma, Y., & Wehrmann, H. (2010). Eruption time series statistically examined:
690 Probabilities of future eruptions at Villarrica and Llaima Volcanoes, South-
691 ern Volcanic Zone, Chile. *Journal of Volcanology and Geothermal Research*,
692 *193*(1), 82–92.
- 693 Endo, E. T., & Murray, T. (1991, September). Real-time Seismic Amplitude Mea-
694 surement (RSAM): a volcano monitoring and prediction tool. *Bulletin of Vol-*
695 *canology*, *53*(7), 533–545. doi: 10.1007/bf00298154
- 696 Galle, B., Johansson, M., Rivera, C., Zhang, Y., Kihlman, M., Kern, C., ... Hidalgo,
697 S. (2010, March). Network for Observation of Volcanic and Atmospheric
698 Change (NOVAC)—A global network for volcanic gas monitoring: Network
699 layout and instrument description. *Journal of Geophysical Research*, *115*(D5).
700 doi: 10.1029/2009jd011823
- 701 Global Volcanism Program. (2013). Villarrica. In E. Venzke (Ed.), *Volcanoes of the*
702 *World, v. 4.4.1*. <http://dx.doi.org/10.5479/si.GVP.VOTW4-2013>: Smithsonian
703 Institution. Retrieved from <http://dx.doi.org/10.5479/si.GVP.VOTW4-2013>
704 (Downloaded 20 Nov 2015)
- 705 Global Volcanism Program. (2014). Report on Villarrica (Chile). *Bulletin of the*
706 *Global Volcanism Network*, *39*(3). doi: 10.5479/si.gvp.bgvn201403-357120
- 707 Goto, A., & Johnson, J. B. (2011, March). Monotonic infrasound and Helmholtz
708 resonance at Volcan Villarrica (Chile). *Geophysical Research Letters*, *38*(6),
709 L06301. Retrieved 2017-08-22, from [http://onlinelibrary.wiley.com/doi/](http://onlinelibrary.wiley.com/doi/10.1029/2011GL046858/abstract)
710 [10.1029/2011GL046858/abstract](http://onlinelibrary.wiley.com/doi/10.1029/2011GL046858/abstract) doi: 10.1029/2011GL046858
- 711 Grainger, J. F., & Ring, J. (1962, February). Anomalous Fraunhofer Line Profiles.
712 *Nature*, *193*(4817), 762–762. doi: 10.1038/193762a0
- 713 Gurioli, L., Harris, A. J. L., Houghton, B. F., Polacci, M., & Ripepe, M. (2008, Au-
714 gust). Textural and geophysical characterization of explosive basaltic activity
715 at Villarrica volcano. *Journal of Geophysical Research: Solid Earth*, *113*(B8),
716 B08206. Retrieved 2017-08-22, from [http://onlinelibrary.wiley.com/doi/](http://onlinelibrary.wiley.com/doi/10.1029/2007JB005328/abstract)
717 [10.1029/2007JB005328/abstract](http://onlinelibrary.wiley.com/doi/10.1029/2007JB005328/abstract) doi: 10.1029/2007JB005328
- 718 Hammer, C., Ohrnberger, M., & Fh, D. (2012, November). Classifying seismic wave-
719 forms from scratch: a case study in the alpine environment. *Geophysical Jour-*
720 *nal International*, *192*(1), 425–439. doi: 10.1093/gji/ggs036
- 721 Ignatieva, A., Bell, A. F., & Worton, B. J. (2018). Point process models for quasi-
722 periodic volcanic earthquakes. Retrieved from [https://arxiv.org/pdf/1803](https://arxiv.org/pdf/1803.07688.pdf)
723 [.07688.pdf](https://arxiv.org/pdf/1803.07688.pdf)
- 724 Jochen Stutz, U. P. (2008). *Differential Optical Absorption Spectroscopy*. Springer-
725 Verlag GmbH. Retrieved from [https://www.ebook.de/de/product/](https://www.ebook.de/de/product/8900321/jochen_stutz_ulrich_platt_differential_optical_absorption_spectroscopy.html)
726 [8900321/jochen_stutz_ulrich_platt_differential_optical_absorption](https://www.ebook.de/de/product/8900321/jochen_stutz_ulrich_platt_differential_optical_absorption_spectroscopy.html)
727 [_spectroscopy.html](https://www.ebook.de/de/product/8900321/jochen_stutz_ulrich_platt_differential_optical_absorption_spectroscopy.html)
- 728 Johansson, M., Galle, B., Zhang, Y., Rivera, C., Chen, D., & Wyser, K. (2009, Jan-
729 uary). The dual-beam mini-DOAS technique—measurements of volcanic gas
730 emission, plume height and plume speed with a single instrument. *Bulletin of*

- 731 *Volcanology*, 71(7), 747–751. doi: 10.1007/s00445-008-0260-8
- 732 la Cruz-Reyna, S. D. (1991, December). Poisson-distributed patterns of ex-
733 plosive eruptive activity. *Bulletin of Volcanology*, 54(1), 57–67. doi:
734 10.1007/bf00278206
- 735 Lehr, J., Eckel, F., Thorwart, M., & Rabbel, W. (2019, November). Low-frequency
736 seismicity at villarrica volcano: Source location and seismic velocities. *Jour-
737 nal of Geophysical Research: Solid Earth*, 124(11), 11505–11530. doi: 10.1029/
738 2018jb017023
- 739 Liu, E. J., Wood, K., Mason, E., Edmonds, M., Aiuppa, A., Giudice, G., . . . Bu-
740 carey, C. (2019, February). Dynamics of outgassing and plume transport
741 revealed by proximal unmanned aerial system (UAS) measurements at volcán
742 villarrica, chile. *Geochemistry, Geophysics, Geosystems*, 20(2), 730–750. doi:
743 10.1029/2018gc007692
- 744 Martino, S. D., Errico, A., Palo, M., & Cimini, G. B. (2012, March). Explosion
745 swarms at Stromboli volcano: a proxy for nonequilibrium conditions in the
746 shallow plumbing system. *Geochemistry, Geophysics, Geosystems*, 13(3),
747 n/a–n/a. doi: 10.1029/2011gc003949
- 748 Marzocchi, W., & Bebbington, M. S. (2012, July). Probabilistic eruption forecasting
749 at short and long time scales. *Bulletin of Volcanology*, 74(8), 1777–1805. doi:
750 10.1007/s00445-012-0633-x
- 751 Mather, T. A., Tsanev, V. I., Pyle, D. M., McGonigle, A. J. S., Oppenheimer, C., &
752 Allen, A. G. (2004, November). Characterization and evolution of tropospheric
753 plumes from Lascar and Villarrica volcanoes, Chile. *Journal of Geophysical
754 Research: Atmospheres*, 109(D21), n/a–n/a. doi: 10.1029/2004jd004934
- 755 Matoza, R. S., & Chouet, B. A. (2010, December). Subevents of long-period seis-
756 micity: Implications for hydrothermal dynamics during the 20042008 eruption
757 of Mount St. Helens. *Journal of Geophysical Research: Solid Earth*, 115(B12),
758 B12206. Retrieved 2017-09-29, from [http://onlinelibrary.wiley.com/doi/
759 10.1029/2010JB007839/abstract](http://onlinelibrary.wiley.com/doi/10.1029/2010JB007839/abstract) doi: 10.1029/2010JB007839
- 760 Molchan, G. (2005, June). Interevent Time Distribution in Seismicity: A The-
761 oretical Approach. *pure and applied geophysics*, 162(6-7), 1135–1150. Re-
762 trieved 2017-10-02, from [https://link.springer.com/article/10.1007/
763 s00024-004-2664-5](https://link.springer.com/article/10.1007/s00024-004-2664-5) doi: 10.1007/s00024-004-2664-5
- 764 Mora-Stock, C. (2015). *Seismic Structure and Seismicity of the Villarrica
765 Volcano, (Southern Central Chile)* (Phd Thesis, Christian-Albrechts-
766 Universität zu Kiel). Retrieved from [http://macau.uni-kiel.de/receive/
767 dissertation_diss_00017649](http://macau.uni-kiel.de/receive/dissertation_diss_00017649)
- 768 Moussallam, Y., Bani, P., Curtis, A., Barnie, T., Moussallam, M., Peters, N., . . .
769 Cardona, C. (2016, November). Sustaining persistent lava lakes: Observations
770 from high-resolution gas measurements at Villarrica volcano, Chile. *Earth and
771 Planetary Science Letters*, 454, 237–247. doi: 10.1016/j.epsl.2016.09.012
- 772 Ortiz, R., Moreno, H., García, A., Fuentealba, G., Astiz, M., Peña, P., . . . Tárraga,
773 M. (2003). Villarrica volcano (Chile): characteristics of the volcanic tremor,
774 and forecasting of small explosions by means of a material failure, method.
775 *Journal of Volcanology and Geothermal Research*, 128(1), 247–259. Re-
776 trieved from [https://www.sciencedirect.com/science/article/pii/
777 S0377027303002580](https://www.sciencedirect.com/science/article/pii/S0377027303002580) doi: [https://doi.org/10.1016/S0377-0273\(03\)00258-0](https://doi.org/10.1016/S0377-0273(03)00258-0)
- 778 Palma, J. L., Blake, S., & Calder, E. S. (2011, November). Constraints on the rates
779 of degassing and convection in basaltic open-vent volcanoes. *Geochemistry,
780 Geophysics, Geosystems*, 12(11), n/a–n/a. doi: 10.1029/2011gc003715
- 781 Palma, J. L., Calder, E. S., Basualto, D., Blake, S., & Rothery, D. A. (2008,
782 October). Correlations between SO₂ flux, seismicity, and outgassing ac-
783 tivity at the open vent of Villarrica volcano, Chile. *Journal of Geophysi-
784 cal Research: Solid Earth*, 113(B10), B10201. Retrieved 2017-08-25, from
785 <http://onlinelibrary.wiley.com/doi/10.1029/2008JB005577/abstract>

- 786 doi: 10.1029/2008JB005577
- 787 Pering, T. D., Tamburello, G., McGonigle, A. J. S., Aiuppa, A., James, M. R., Lane,
788 S. J., ... Patanè, D. (2015, July). Dynamics of mild strombolian activity on
789 Mt. Etna. *Journal of Volcanology and Geothermal Research*, 300, 103–111.
790 doi: 10.1016/j.jvolgeores.2014.12.013
- 791 Platt, U., Bobrowski, N., & Butz, A. (2018, January). Ground- Based Re-
792 mote Sensing and Imaging of Volcanic Gases and Quantitative Determi-
793 nation of Multi-Species Emission Fluxes. *Geosciences*, 8(2), 44. doi:
794 10.3390/geosciences8020044
- 795 Rabbel, W., & Thorwart, M. (2019). *Villarrica Tomography (VITO)* (Dataset). GFZ
796 Data Services. doi: <http://doi.org/10.5880/GIPP.201202.1>
- 797 Richardson, J. P., & Waite, G. P. (2013). Waveform inversion of shallow
798 repetitive long period events at Villarrica, Volcano, Chile. *Journal of*
799 *Geophysical Research: Solid Earth*, 118(9), 4922–4936. Retrieved from
800 <http://onlinelibrary.wiley.com/doi/10.1002/jgrb.50354/full> doi:
801 <https://doi.org/10.1002/jgrb.50354>
- 802 Richardson, J. P., Waite, G. P., & Palma, J. L. (2014). Varying seismic-acoustic
803 properties of the fluctuating lava lake, at Villarrica Volcano, Chile. *Journal*
804 *of Geophysical Research: Solid Earth*, 119(7), 5560–5573. Retrieved from
805 <https://agupubs.onlinelibrary.wiley.com/doi/10.1002/2014JB011002>
806 doi: <https://doi.org/10.1002/2014JB011002>
- 807 Ripepe, M., & Marchetti, E. (2002, November). Array tracking of infrasonic sources
808 at Stromboli volcano. *Geophysical Research Letters*, 29(22), 33–1. Retrieved
809 2018-04-25, from [https://agupubs.onlinelibrary.wiley.com/doi/full/](https://agupubs.onlinelibrary.wiley.com/doi/full/10.1029/2002GL015452)
810 [10.1029/2002GL015452](https://doi.org/10.1029/2002GL015452) doi: 10.1029/2002GL015452
- 811 Ripepe, M., Marchetti, E., Bonadonna, C., Harris, A. J. L., Pioli, L., & Ulivieri,
812 G. (2010, August). Monochromatic infrasonic tremor driven by persis-
813 tent degassing and convection at Villarrica Volcano, Chile. *Geophysical*
814 *Research Letters*, 37(15), L15303. Retrieved 2017-08-22, from [http://](http://onlinelibrary.wiley.com/doi/10.1029/2010GL043516/abstract)
815 onlinelibrary.wiley.com/doi/10.1029/2010GL043516/abstract doi:
816 [10.1029/2010GL043516](https://doi.org/10.1029/2010GL043516)
- 817 Saichev, A., & Sornette, D. (2006, August). Universal distribution of in-
818 terearthquake times explained. *Physical Review Letters*, 97(7). doi:
819 [10.1103/physrevlett.97.078501](https://doi.org/10.1103/physrevlett.97.078501)
- 820 Salerno, G. G., Burton, M., Grazia, G. D., Caltabiano, T., & Oppenheimer, C.
821 (2018, oct). Coupling between magmatic degassing and volcanic tremor
822 in basaltic volcanism. *Frontiers in Earth Science*, 6. doi: 10.3389/
823 feart.2018.00157
- 824 Sanchez, L., & Shcherbakov, R. (2012, December). Temporal scaling of volcanic
825 eruptions. *Journal of Volcanology and Geothermal Research*, 247-248, 115–
826 121. Retrieved 2018-03-15, from [http://www.sciencedirect.com/science/](http://www.sciencedirect.com/science/article/pii/S0377027312002429)
827 [article/pii/S0377027312002429](http://www.sciencedirect.com/science/article/pii/S0377027312002429) doi: 10.1016/j.jvolgeores.2012.08.004
- 828 Taddeucci, J., Palladino, D. M., Sottili, G., Bernini, D., Andronico, D., & Cristaldi,
829 A. (2013, July). Linked frequency and intensity of persistent volcanic activity
830 at stromboli (italy). *Geophysical Research Letters*, 40(13), 3384–3388. doi:
831 [10.1002/grl.50652](https://doi.org/10.1002/grl.50652)
- 832 Touati, S., Naylor, M., & Main, I. G. (2009, April). Origin and Nonuniversality
833 of the Earthquake Interevent Time Distribution. *Physical Review Letters*,
834 102(16), 168501. Retrieved 2017-11-13, from [https://link.aps.org/doi/](https://link.aps.org/doi/10.1103/PhysRevLett.102.168501)
835 [10.1103/PhysRevLett.102.168501](https://link.aps.org/doi/10.1103/PhysRevLett.102.168501) doi: 10.1103/PhysRevLett.102.168501
- 836 Traversa, P., & Grasso, J.-R. (2010, August). How is Volcano Seismicity Dif-
837 ferent from Tectonic Seismicity? *Bulletin of the Seismological Society*
838 *of America*, 100(4), 1755–1769. Retrieved 2017-09-29, from [https://](https://pubs.geoscienceworld.org/bssa/article/100/4/1755/349480/how-is-volcano-seismicity-different-from-tectonic)
839 [pubs.geoscienceworld.org/bssa/article/100/4/1755/349480/how-is](https://pubs.geoscienceworld.org/bssa/article/100/4/1755/349480/how-is-volcano-seismicity-different-from-tectonic)
840 [-volcano-seismicity-different-from-tectonic](https://pubs.geoscienceworld.org/bssa/article/100/4/1755/349480/how-is-volcano-seismicity-different-from-tectonic) doi: 10.1785/0120090214

- 841 Vandaele, A. C., Simon, P. C., Guilmot, J. M., Carleer, M., & Colin, R. (1994).
842 SO₂absorption cross section measurement in the UV using a Fourier trans-
843 form spectrometer. *Journal of Geophysical Research*, *99*(D12), 25599. doi:
844 10.1029/94jd02187
- 845 Varley, N., Johnson, J., Ruiz, M., Reyes, G., Martin, K., de Ciencias, F., & Col-
846 ima, M. (2006). Applying statistical analysis to understanding the dy-
847 namics of volcanic explosions. In *Statistics in volcanology* (Vol. 1, pp. 57–
848 76). Citeseer. Retrieved from [http://citeseerx.ist.psu.edu/viewdoc/
849 download?doi=10.1.1.521.1265&rep=rep1&type=pdf](http://citeseerx.ist.psu.edu/viewdoc/download?doi=10.1.1.521.1265&rep=rep1&type=pdf)
- 850 Voigt, S., Orphal, J., Bogumil, K., & Burrows, J. P. (2001, October). The tem-
851 perature dependence (203–293 K) of the absorption cross sections of O₃ in
852 the 230–850 nm region measured by Fourier-transform spectroscopy. *Jour-
853 nal of Photochemistry and Photobiology A: Chemistry*, *143*(1), 1–9. doi:
854 10.1016/s1010-6030(01)00480-4
- 855 Witter, J. B., Kress, V. C., Delmelle, P., & Stix, J. (2004, July). Volatile degassing,
856 petrology, and magma dynamics of the Villarrica Lava Lake, Southern Chile.
857 *Journal of Volcanology and Geothermal Research*, *134*(4), 303–337. Retrieved
858 2017-08-25, from [http://www.sciencedirect.com/science/article/pii/
859 S0377027304000630](http://www.sciencedirect.com/science/article/pii/S0377027304000630) doi: 10.1016/j.jvolgeores.2004.03.002